

Computational Methods in Quantum Field Theory

Kurt Langfeld

School of Mathematics & Statistics, University of Plymouth
Plymouth, PL4 8AA, UK
email: kurt.langfeld@plymouth.ac.uk

October 11, 2007

Abstract

Lecture notes (0-12h).

Contents

1	Statistical data analysis	3
1.1	The Central Limit Theorem	3
1.2	Error analysis	7
1.3	Autocorrelations	9
2	Lessons from the Ising model	11
2.1	Phase transitions	11
2.2	Quantum field theory rising	12
2.3	Mean-field approximation	14
2.4	Duality transformation	17
3	Markov chain Monte-Carlo: the Ising case study	21
3.1	Foundations	21
3.2	Heat-bath algorithm	24
3.3	Cluster update algorithms	26
4	Quantum field theories on computers	27
4.1	Quantum Mechanics	27
4.2	Quantum field theory	30
5	Lattice gauge theory	31
5.1	The gauged Ising model	31
5.2	Setting up lattice Yang-Mills theory	34
5.3	The fermion doubling problem	38
5.4	Overlap Fermions	41
5.5	Measuring observables	42
5.6	The continuum limit	43

1 Statistical data analysis

1.1 The Central Limit Theorem

Assume that we would like to determine a physical observable \bar{x} such as a hadron mass or a decay constant by a numerical calculation involving statistical methods or by a direct experimental measurement. In both cases, we obtain an estimate x for \bar{x} . Let $P(x) dx$ be the probability to obtain a particular value within the interval $[x, x + dx]$. On average, the measurements will reproduce the observable, i.e.,

$$\int dx x P(x) = \bar{x}, \quad (1)$$

but, depending on $P(x)$, a single measurement can be far off the true value.

As an example, we consider an observable $\bar{x} = 3$ and a crude experimental which can produce any value for between 0 and 6 with equal probability:

$$P(x) = \begin{cases} 1/6 & \text{for } x \in [0, 6] \\ 0 & \text{otherwise.} \end{cases} \quad (2)$$

Obviously, a single measurement for x is not sufficient to reveal the true observable since a measurement could produce any value between 0 and 6. The only thing we can do is to repeat the measurement n times and to consider the average:

$$y = \frac{1}{n} [x_1 + \dots + x_n],$$

where x_1 to x_n are the values obtained from each of the measurements. For the moment, we will assume that the measurements are *independent*, i.e., that the probability for finding a set $\{x_1 \dots x_n\}$ of data is given by:

$$P(x_1, \dots, x_n) = P(x_1) \dots P(x_n).$$

The crucial question is, however, to which accuracy we have estimated the true observable \bar{x} ?

The answer can be inferred from the probability distribution $Q(y)$ for the value y is:

$$Q_n(y) = \int \prod_{i=1}^n dx_i \delta\left(y - \frac{1}{n} [x_1 + \dots + x_n]\right) P(x_1) \dots P(x_n). \quad (3)$$

Given the proper normalisation of the single event distributions, i.e.,

$$\int dx_i P(x_i) = 1,$$

and using (1), we easily show that the average of y coincides with the observable:

$$\begin{aligned}\bar{y} &= \int dy y Q_n(y) \\ &= \int dy \int \prod_{i=1}^n dx_i \frac{1}{n} [x_1 + \dots + x_n] \delta\left(y - \frac{1}{n} [x_1 + \dots + x_n]\right) P(x_1) \dots P(x_n) . \\ &= \int \prod_{i=1}^n dx_i \frac{1}{n} [x_1 + \dots + x_n] P(x_1) \dots P(x_n) = \frac{1}{n} n \int dx x P(x) = \bar{x} .\end{aligned}$$

A natural measure for the error σ of our estimate is provided by the second moment:

$$\sigma^2(n) = \int dy (y - \bar{y})^2 Q_n(y) . \quad (4)$$

If the distribution $Q_n(y)$ peaks around the true value for our observable \bar{x} and $\sigma(n)$ is tiny, it would mean that already one estimator y is bound to fall close to \bar{x} with high probability implying that it yields a good approximation to \bar{x} .

Let us study for this reason the moments of the distribution $Q(y)$:

$$q_m = \int dy Q_n(y) y^m . \quad (5)$$

In order to draw further conclusions, we need to restrict the classes of single event probability distributions $P(x)$: we will assume that its Fourier transform

$$\bar{P}(\beta) = \int dx P(x) \exp\{-i\beta x\} \quad (6)$$

is an analytic function of β at $\beta = 0$. As a consequence, the moments of $P(x)$ exist and are given by:

$$p_m = \int dx P(x) x^m = i^m \frac{d^m}{d\beta^m} \bar{P}(\beta) |_{\beta=0} . \quad (7)$$

We will further assume that $\bar{P}(\beta)$ vanishes for $|\beta| \rightarrow \pm\infty$. This seems to be quite a weak constraint. I point out, however, that systems with rare but large fluctuations generical fail to possess higher moments. One example are stock market indices.

Our aim is to express the moments of $Q_n(y)$ in terms of the moments of $P(x)$. For this purpose, we rewrite the δ -function in (3) as

$$\delta\left(y - \frac{1}{n} [x_1 + \dots + x_n]\right) = \int \frac{d\alpha}{2\pi} \exp[i\alpha y] \prod_{i=1}^n \exp\left\{-i\frac{\alpha}{n} x_i\right\} , \quad (8)$$

and find

$$Q_n(y) = \int \frac{d\alpha}{2\pi} \exp(i\alpha y) \left[\int dx P(x) \exp\left\{-i\frac{\alpha}{n} x\right\} \right]^n , \quad (9)$$

$$= \int \frac{d\alpha}{2\pi} \exp(i\alpha y) \left[\bar{P}\left(\frac{\alpha}{n}\right) \right]^n . \quad (10)$$

The moments of $Q_n(y)$ are then obtained from

$$q_m = \int dy \int \frac{d\alpha}{2\pi} (-i)^m \frac{d^m}{d\alpha^m} \left[\exp(i\alpha y) \right] \bar{P}^n \left(\frac{\alpha}{n} \right). \quad (11)$$

After a series of partial integrations with vanishing boundary terms, the latter equation is given by

$$\begin{aligned} q_m &= \int dy \int \frac{d\alpha}{2\pi} \exp(i\alpha y) (i)^m \frac{d^m}{d\alpha^m} \left[\bar{P}^n \left(\frac{\alpha}{n} \right) \right] \\ &= \int \frac{d\alpha}{2\pi} \frac{1}{n^m} \int dy \exp(i\alpha y) (i)^m \frac{d^m}{d\beta^m} \left[\bar{P}^n(\beta) \right] = \frac{i^m}{n^m} \frac{d^m}{d\beta^m} \left[\bar{P}^n(\beta) \right] \Big|_{\beta=0}. \end{aligned} \quad (12)$$

Of particular interest are the so-called cummulants $c_k[Q_n]$ of the distribution $Q_n(y)$. These are defined via the generating function

$$T_Q(x) = \sum_{m=0}^{\infty} \frac{1}{m!} q_m x^m, \quad c_k[Q_n] := \frac{d^k}{dx^k} \ln T_Q(x) \Big|_{x=0}. \quad (13)$$

Note that in particular we find for the 'error' σ in (4)

$$\sigma^2 = q_2 - q_1^2 = c_2[Q_n]. \quad (14)$$

Using Taylor's theorem and the explicit expression (12), we find

$$T_Q(x) = \bar{P}^n \left(\frac{ix}{n} \right), \quad c_k[Q_n] = \frac{i^k}{n^{k-1}} \left[\ln \bar{P}(0) \right]^{(k)}. \quad (15)$$

Introducing the cummulants $c_k[P]$ of the single event distribution as well, i.e.,

$$c_k[P] = i^k \left[\ln \bar{P}(0) \right]^{(k)}, \quad (16)$$

we arrive at a very important result:

$$c_k[Q_n] = \frac{1}{n^{k-1}} c_k[P]. \quad (17)$$

Note that the cummulants $c_k[P]$ are finite numbers which characterise the single event probability distribution. The latter equation then implies that for increasing number of measurements n , the higher ($k > 1$) cummulants of $Q_n(y)$ vanish. In particular, we find that

$$\sigma(n) = \sqrt{c_2[Q_n]} = \frac{\sqrt{c_2[P]}}{\sqrt{n}} \propto 1/\sqrt{n}. \quad (18)$$

For the above example, we find

$$p_1 = \frac{1}{6} \int_0^6 dx x = 3, \quad p_2 = \frac{1}{6} \int_0^6 dx x^2 = 12, \quad c_2[P] = 12 - 3^2 = 3, \quad (19)$$

and therefore

$$\sigma(n) = \sqrt{3/n}.$$

It is well known that if $c_k[G] = 0$ for $k > 2$, the probability distribution G is a Gaussian. We therefore expect that if n is chosen such large that we can neglect $c_k[Q_n]$ with $k > 2$, we should be able to approximate $Q_n(y)$ by a Gaussian. To support this claim (without mathematical rigour), we start from (10):

$$Q_n(y) = \int \frac{d\alpha}{2\pi} \exp(i\alpha y) \exp \left\{ n \ln \left[\bar{P} \left(\frac{\alpha}{n} \right) \right] \right\},$$

and expand the logarithm with respect to α :

$$\begin{aligned} Q_n(y) &= \int \frac{d\alpha}{2\pi} \exp(i\alpha y) \exp \left\{ n \sum_{k=0}^{\infty} \frac{1}{k!} [\ln \bar{P}(0)]^{(k)} \left(\frac{\alpha}{n} \right)^k \right\} \\ &= \int \frac{d\alpha}{2\pi} \exp(i\alpha y) \exp \left\{ n \sum_{k=1}^{\infty} \frac{1}{k!} c_k[P] \left(-i \frac{\alpha}{n} \right)^k \right\}, \end{aligned}$$

where we have used $\bar{P}(0) = \int dx P(x) = 1$ and the definition of the cummulants of P in (16). Using $c_1[P] = p_1 = \bar{x} = \bar{y}$, we find:

$$Q_n(y) = \int \frac{d\alpha}{2\pi} \exp[i\alpha(y - \bar{y})] \exp \left\{ -\frac{1}{2} c_2[P] \left(\frac{\alpha^2}{n} \right) + \mathcal{O}(\alpha^3/n^2) \right\} \quad (20)$$

Note that the dominant contributions from the α integration arises from the regime where $\alpha < \sqrt{n}$. In this regime, the correction term is of order

$$\mathcal{O}(\alpha^3/n^2) \approx \mathcal{O}(1/\sqrt{n})$$

and will be neglected for sufficiently large n . The remaining integral can be easily performed:

$$Q_n(y) \approx \frac{1}{\sqrt{2\pi}\sigma} \exp \left\{ -\frac{(y - \bar{y})^2}{2\sigma^2} \right\}, \quad \sigma^2 = \frac{c_2[P]}{n}. \quad (21)$$

which is the celebrated Gaussian distribution.

Let us discuss the result...

The existence of at least the moment $c_2[P]$ of the single event distribution is crucial for the error reduction by repeated measurements. Let us consider a Lorentz distribution for the moment:

$$P_L(x) = \frac{1}{\pi b} \frac{1}{1 + (x/b)^2}. \quad (22)$$

With the naked eye this distribution is not so much different from the Gaussian. The crucial difference is, however, that the second moment does not exist:

$$\int dx x^2 P_L(x) \longrightarrow \infty.$$

The Fourier transform of $P_L(x)$ does exist, i.e.,

$$\bar{P}_L(\beta) = \exp\{-b|\beta|\} . \quad (23)$$

If we now repeat the measurements n times, the distribution of the average y is given according to (10) by

$$Q_n(y) = \int \frac{d\alpha}{2\pi} \exp(i\alpha y) \left[\exp\left(-b\frac{\alpha}{n}\right) \right]^n = P_L(y) .$$

Obviously, the probability distribution does not change at all even if we repeat the measurements many times. This actually implies that it is impossible to experimentally gain a reliable value for the observable \bar{x} .

1.2 Error analysis

Let us return to the example in (2), and let us assume a group of experimentalists has performed $n = 12$ measurements with the result:

$$\begin{array}{cccc} 2.813 & 2.021 & 0.331 & 0.865 \\ 5.394 & 5.937 & 5.027 & 1.556 \\ 0.325 & 2.750 & 1.283 & 3.890 \end{array}$$

The average over these values and an estimate $\langle x^2 \rangle$ of $c_2[P]$ are given by

$$y = \frac{1}{n} \sum_{k=1}^n x_k \approx 2.683 , \quad \langle x^2 \rangle = \frac{1}{n} \sum_{k=1}^n x_k^2 \approx 3.581 . \quad (24)$$

Note that 3.581 is a pure estimate of the true value (19) of $c_2[P] = 3$, but it reflects the order of magnitude. With this estimate for $c_2[P]$, we find for the error (18)

$$\sigma(n=12) \approx \sqrt{\frac{3.581}{12}} \approx 0.546 .$$

Hence, the final 'experimental' result for the observable would be

$$\bar{x} \approx 2.683 \pm 0.581 = 2.7(6) . \quad (25)$$

Note that the true result $\bar{x} = 3$ lies well within the reach of the error bars.

The above experiment was repeated by several research labs. Depending on the budget and the focal point of research, different labs produce different numbers n of measurements:

	CERN	GSI	DESY	BNL
n	120	50	78	150
y	3.112 ± 0.163	2.764 ± 0.255	3.110 ± 0.207	3.083 ± 0.143

The smallest error was produced by the biggest experiment (BNL). We could just quote their result, but it would be a pity to disregard a total of 248 measurements which were carried out by the other groups. How can we obtain a 'world average' for the observable \bar{x} and how can we quantify its (statistical) error?

To answer these questions, we assume that the number n of each measurement was large enough to approximate the distribution of an individual result y_k , $k = 1 \dots N$ (where $N = 4$ for the above example) by a Gaussian (21):

$$Q(y_l) \approx \frac{1}{\sqrt{2\pi} \sigma_l} \exp \left\{ -\frac{(y_l - \bar{x})^2}{2\sigma_l^2} \right\}. \quad (26)$$

For the world average y we make the ansatz

$$y = \sum_{l=1}^N a_l y_l, \quad \sum_{l=1}^N a_l = 1. \quad (27)$$

The weights a_l must be chosen in an optimal way. This choice will depend on the errors σ_l of the individual experiments. In particular, the experiment with the smallest error should contribute to the world average with the largest weight. Assuming that the experiments at the different labs were carried out independently, the probability distribution of the world average is now given by

$$W(y) = \int \prod_{k=1}^N dy_k \delta\left(y = \sum_{l=1}^N a_l y_l\right) Q(y_1) \dots Q(y_N). \quad (28)$$

Representing the δ -function in terms of a Fourier integral over α (see (8)), the integrations over $dy_1 \dots dy_N$ can be easily performed:

$$W(y) = \int \frac{d\alpha}{2\pi} \exp\{i(y - \bar{x})\alpha\} \exp \left\{ -\frac{\alpha^2}{2} \sum_l a_l^2 \sigma_l^2 \right\}.$$

Performing the α integration finally yields:

$$Q(y) \approx \frac{1}{\sqrt{2\pi} \sigma} \exp \left\{ -\frac{(y - \bar{x})^2}{2\sigma^2} \right\}, \quad \sigma^2 = \sum_l a_l^2 \sigma_l^2. \quad (29)$$

The optimal result is achieved if the error squared, i.e., σ^2 , is as small as possible. Thereby, we must take into account the normalisation condition in (27). We therefore minimise

$$\sum_l \left[a_l^2 \sigma_l^2 - \lambda a_l \right] \longrightarrow \min, \quad (30)$$

where λ is a Lagrange multiplier. The global minimum is easily obtained:

$$a_l = \frac{\lambda}{2\sigma_l^2}, \quad \frac{2}{\lambda} = \sum_l \frac{1}{\sigma_l^2}. \quad (31)$$

The minimal value for σ^2 then satisfies

$$\sigma^2 = \frac{\lambda}{2} \quad \Rightarrow \quad \frac{1}{\sigma^2} = \sum_l \frac{1}{\sigma_l^2} . \quad (32)$$

The optimal choice for the weights can therefore also be written as

$$a_l = \frac{\sigma^2}{\sigma_l^2} . \quad (33)$$

Let us return to the above example. We find

$$\begin{aligned} \sigma &\approx 0.089 , \\ a_1 &\approx 0.30 , \quad a_2 \approx 0.12 , \quad a_3 \approx 0.19 , \quad a_4 \approx 0.39 . \end{aligned} \quad (34)$$

With the weights at our disposal, we easily find the optimal value for the world average $y \approx 3.059$. Together with the error in (34), the final result is

$$\bar{x} = 3.059 \pm 0.089 = 3.06(9) . \quad (35)$$

Note that the true result $\bar{x} = 3$ is again covered within error bars and that the error became significantly smaller than that of the best result provided by the BNL group.

1.3 Autocorrelations

In the previous subsections, we have repeatedly used that the measurements x_i are independent. We will see below that a vital tool of computational quantum field theory is to use information from the measurement x_i to obtain the value for x_{i+1} . In this case, the data set x_i , $i = 1 \dots n$ is generated by the chain

$$x_1 \rightarrow x_2 \rightarrow \dots \rightarrow x_{n-1} \rightarrow x_n ,$$

and the probability of finding a particular set does not factorise anymore:

$$P(x_1, \dots, x_n) \neq P(x_1) \dots P(x_n) .$$

In the context of QFT simulations we will make, however, an effort to make the values x_i as independent as possible. This generically implies that events which are separated by some 'time' τ , i.e., the events x_i and $x_{i+\tau}$, can be considered as statistically independent. The trick for obtaining an idea of the error of the estimator is to group b measurements together:

$$y_\nu = \frac{1}{b} \sum_{i=1}^b x_{\nu+i} , \quad \nu = 1 \dots M , \quad M = \frac{n}{b} . \quad (36)$$

Thereby we choose

$$1 \leq \tau \ll b . \quad (37)$$

This choice guarantees that the values y_ν are statistically independent and that these values are Gaussian distributed because of the central limit theorem. The quantity of interest are the average

$$\bar{y} = \frac{1}{M} \sum_{\nu=1}^M y_\nu, \quad (38)$$

which converges to the observable \bar{x} in the limit $M \rightarrow \infty$, and the corresponding error

$$\sigma^2 = \frac{1}{M} c_2[P_y] = \frac{b}{n} c_2[P_y]. \quad (39)$$

where the cumulant $c_2[P_y]$ is given by

$$c_2[P_y] = \left\langle \frac{1}{M} \sum_{\nu=1}^M y_\nu^2 \right\rangle - \left[\left\langle \frac{1}{M} \sum_{\nu=1}^M y_\nu \right\rangle \right]^2, \quad (40)$$

where

$$\langle f \rangle = \int \prod_{l=1}^n dx_l f(x_1 \dots x_n) P(x_1, \dots, x_n).$$

Assuming translational invariance, i.e.,

$$\langle x_{\nu+i} x_{\nu+k} \rangle = \langle x_i x_k \rangle,$$

we find

$$c_2[P_y] = \frac{1}{b^2} \sum_{i=1}^b \sum_{k=1}^b c(k-i), \quad c(k-i) = \langle x_i x_k \rangle - \langle x_i \rangle \langle x_k \rangle, \quad (41)$$

where $c(k-i)$ is called *autocorrelation function*. Introducing the relative distance $t = k-i$, and trading the summation over k in (41) for a summation over t , we find

$$c_2[P_y] = \frac{1}{b^2} \sum_{i=1}^b \sum_{t=1-i}^{b-i} c(t). \quad (42)$$

Interchanging the summation indices t and i and after summing over i , the latter equation becomes:

$$c_2[P_y] = \frac{1}{b} c(0) + \frac{2}{b^2} \sum_{t=1}^{b-1} (b-t) c(t).$$

We have already mentioned that the measurements x_i and $x_{i+\tau}$ are (almost) uncorrelated. The equivalent statement is that the correlation function vanishes for sufficiently large arguments:

$$c(t) \approx 0, \quad \text{for } t > \tau.$$

For $b \gg \tau$, we approximately find:

$$c_2[P_y] \approx \frac{1}{b}c(0) + \frac{2}{b^2} \sum_{t=1}^{b-1} b c(t) = \frac{1}{b} \sum_{t=1-b}^{b-1} c(t). \quad (43)$$

It is convenient to introduce the *normalised autocorrelation function* by

$$\rho(t) = \frac{c(t)}{c(0)}, \quad c(0) = \langle x^2 \rangle - \langle x \rangle^2 = c_2[P_x]. \quad (44)$$

The *integrated autocorrelation time* is then defined by

$$\tau = \frac{1}{2} \sum_{t=1-b}^{b-1} \rho(t) = \frac{1}{2} + \sum_{t=1}^{b-1} \rho(t). \quad (45)$$

Inserting (45,44,43) into (39), we finally obtain for the error which is attributed to our estimate \bar{y} in (38):

$$\sigma^2 = \frac{2\tau}{n} c_2[P_x]. \quad (46)$$

Let us perform a consistency check by considering the special case that the measurements are uncorrelated. In this case, the autocorrelation function $\rho(t)$ vanishes for $t \geq 1$, and the autocorrelation time is given by $\tau = 1/2$. We indeed recover the familiar result

$$\sigma^2 = \frac{1}{n} c_2[P_x], \quad \text{for independent measurements.} \quad (47)$$

Note that autocorrelation increase the error bars. Not knowing the autocorrelations in a numerical simulations leads us to the erroneous assumption that the error of the estimator is given by (47), while the true result is by a factor τ larger. Not knowing the autocorrelations always leads to an underestimation of the statistical error.

2 Lessons from the Ising model

2.1 Phase transitions

A phase transition occurs if the properties of matter change qualitatively when an external parameter, such as temperature, is altered. The phase transition of water from a liquid phase to a gas phase when the temperature exceeds roughly $\approx 100^0 C$ (under normal conditions), is well known from everyday life. A second example is the ferromagnet: the interaction between microscopic spins favour a unique orientation of the spins. This yields an *ordered phase* at small temperatures. Above the critical temperature, called *Curie temperature* in the present context, the spins are organised in a *disordered phase*.

Let us assume that a ferromagnet is in the disordered phase at a temperature slightly bigger than the critical temperature T_c . If we decrease the temperature, the information

of the unique orientation spreads over the spin lattice. This ‘Gedankenexperiment’ shows that the spatial correlation of the spins becomes large at the critical temperature. This phenomenon, is quantified with the help of the so-called *correlation function*:

$$\left\langle \sigma(x) \sigma(y) \right\rangle \propto \exp \left\{ -\frac{|x-y|}{\xi} \right\}. \quad (48)$$

The *correlation length* ξ is obviously a measure for the spatial distance over which the spins show roughly the same orientation. Close to the phase transition, i.e. for $T \lesssim T_c$, ξ becomes large anticipating the ordered phase:

$$\xi \approx \xi_+ \left| 1 - \frac{T}{T_c} \right|^{-\nu}, \quad (T \gtrsim T_c), \quad (49)$$

where ν is a positive number. The divergence of the correlation length at the phase transition is characteristic for a transition of *2nd order* (or higher order). In the case of a *1st order* transition, the increase of ξ is hindered by the nucleation of bubbles which contain chunks of the new state of matter. These bubbles provide additional disorder and the correlation length stays finite.

For phase transitions of higher order than first order, the singularity of the correlation length has its fingerprint in many other thermodynamical quantities such as the *specific heat* C of the *magnetic susceptibility* χ :

$$C \approx C_0 \left| 1 - \frac{T}{T_c} \right|^{-\alpha}, \quad \chi \approx \chi_0 \left| 1 - \frac{T}{T_c} \right|^{-\gamma}, \quad (T \gtrsim T_c).$$

The so-called *critical exponents* ν, α, γ are independent of the microscopic properties of the spin model (such as the lattice geometry), and only depend on the symmetries (present at the transition) and the number of dimensions. They are often used to sort solid state physics models into the so-called *universality classes*.

2.2 Quantum field theory rising

Let us denote the distance a between to sites of the lattice *lattice spacing*. In the previous subsection, we found that the correlation length diverges if the coupling constant β (or inverse temperature in the present context) approaches the critical value (see (49)). This statement can be phrased in units of the lattice spacing as

$$\frac{\xi}{a} = \kappa \left(\beta_c - \beta \right)^{-\nu}, \quad \beta \lesssim \beta_c, \quad (50)$$

where κ is a dimensionless constant which can be calculated by numerical simulations.

Let us now reinterpret these findings. Rather than saying that ξ diverges and a is fixed, we say that the correlation length ξ is fixed and given by an observable in physical units.

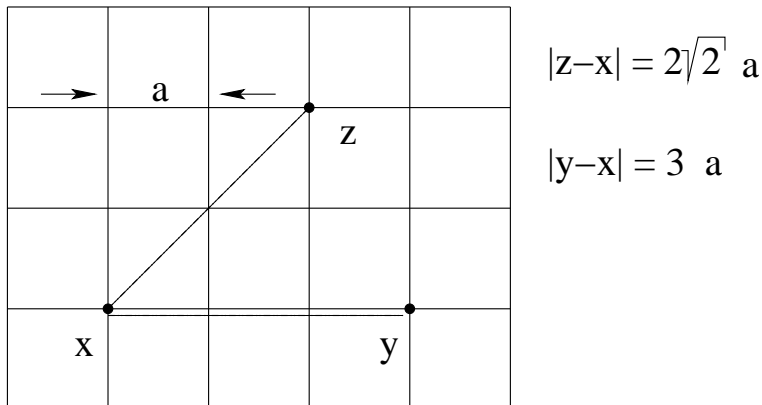


Figure 1: Spin correlation along the diagonal and the symmetry axis, respectively.

According to (50), we also say that now the lattice spacing depends on β . We will see that this interpretation of the same data defines a **quantum field theory**. For fixed correlation length ξ , (50) defines the lattice spacing as a function of β , i.e., $a \rightarrow a(\beta)$,

$$a(\beta) = \frac{1}{\kappa} (\beta - \beta_c)^\nu \xi. \quad (51)$$

The key point is if we make the number of spins bigger and bigger and, at the same time, the distant a between the spins smaller and smaller, we will obtain a field theory in the limit $a \rightarrow 0$. In the Ising case ($\nu = 1$), we obtain the field theory limit if β approaches 0.44... when a linearly vanishes with $\beta - \beta_c$.

Note that the dimensionless parameter β is not at our disposal anymore, since it specifies the magnitude of the lattice spacing. Instead of, the value of ξ is the new parameter of the emerging quantum field theory. The exchange of a dimensionless parameter for a scale dependent one in the case of the quantum field theory is known as *dimensional transmutation*.. It is a generic feature of quantum field theories. For instance in the case of perturbative QCD, the dimensionless gauge coupling g is eliminated in favour of the scale dependent parameter Λ_{QCD} .

Let us assume that a certain correlation function was obtained by a numerical simulation of a classical lattice model,

$$D(|x - y|) = \left\langle F(\phi(x)) F(\phi(y)) \right\rangle \propto \exp\left\{-m|x - y|\right\}, \quad (52)$$

where m is called **screening mass**. Since the distance $|x - y|$ is only known in units of the lattice spacing by construction, the simulation will provide the mass in units of the lattice spacing as function of β , i.e. $ma(\beta)$. If universality holds, one finds the characteristic scaling of the lattice model, i.e.,

$$ma(\beta) = \kappa_m \left(\beta_c - \beta\right)^\nu, \quad \beta \lesssim \beta_c. \quad (53)$$

Hence, the product $m\xi$ approaches a constant in the vicinity of the critical limit, i.e.,

$$m\xi = ma \frac{\xi}{a} = \kappa_m \kappa . \quad (54)$$

Note that κ and κ_m are two c-numbers which we can extract from the numerical simulation. With help of these two numbers we can “measure” the desired mass m in units of $1/\xi$, where ξ is the only free parameter of our theory.

In the case of a quantum field theory, we expect that due to the isotropy of the vacuum the correlation function (52) only depends on the distance between x and y . In the classical lattice model, the rotational symmetry is lost due to the presence of the cubic lattice, and one must fear that the quantum field theory which inherits from the classical lattice model inherits an anisotropy. The hope is that in view of universality, the rotational symmetry is restored in the critical limit (51). Let us investigate this restoration in the case of the 2-dimensional classical Ising model. For this purpose, we compare the correlation length in lattice units along a lattice symmetry axis, ξ , and a long the diagonal direction, ξ_d (see figure 1). One finds (see e.g. [1])

$$\frac{\xi}{\xi_d} = \sqrt{2} \ln\left(\frac{2v}{1-v^2}\right) / \ln\left(v \frac{1+v}{1-v^2}\right), \quad v = \tanh \beta . \quad (55)$$

Some values for the above ratio are shown in table below:

$\beta_c - \beta$	ξ/ξ_d	ξ/a
0.39	1.12	0.35
0.34	1.08	0.48
0.24	1.03	0.83
0.13	1.01	1.71

2.3 Mean-field approximation

Starting point for a thermodynamical description of the Ising model is the partition function:

$$\mathcal{Z} = \sum_{\{\sigma_x\}} \exp(-\beta H(\sigma)) \quad (56)$$

where $\beta = 1/T$ and where a *spin* $\sigma_x = \pm 1$ is associated with each site x of the square lattice. The sum in (56) extends over all possible spin configurations. The *ferromagnetic* interaction favours a unique orientation of the spins, and is described by

$$H(\sigma) = - \sum_{\langle xy \rangle} \sigma_x \sigma_y , \quad (57)$$

where the sum extends over all pairs $\langle xy \rangle$ of nearest neighbours. In order to preserve translational invariance, periodic boundary conditions are often used in particle physics

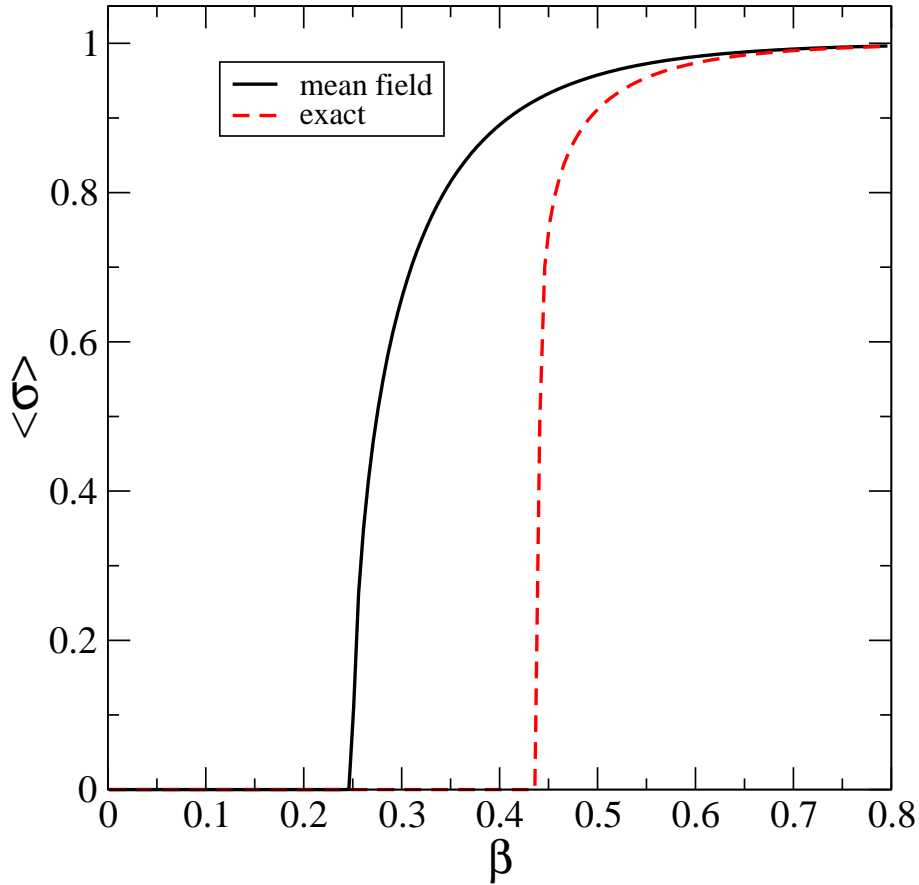


Figure 2: Magnetisation per site as function of the inverse temperature β ; solid line: mean field approximation; dashed line: exact

applications, although these conditions are difficult to interpret in the solid state physics context.

In order to gain first insights into the phase structure of the Ising model, we choose a particular spin of the lattice, and assume heuristically that that we might replace the neighbouring spins by the mean field

$$\langle \sigma \rangle = \frac{1}{\mathcal{Z}} \sum_{\{\sigma_x\}} \sigma_{x_0} \exp(-\beta H(\sigma)) . \quad (58)$$

The Hamiltonian is then approximately given by

$$H(\sigma_{x_0}) \approx \text{const.} - 4\langle \sigma \rangle \sigma_{x_0} . \quad (59)$$

Note that each spin possesses 4 neighbours on a cubic 2d square lattice. Equation (58) turns into a self-consistency equation to determine the $\langle \sigma \rangle$, which can be interpreted as

the magnetisation per site:

$$\langle \sigma \rangle = \frac{1}{\mathcal{N}} \sum_{\sigma_{x_0}=\pm 1} \sigma_{x_0} \exp(-\beta H(\sigma)), \quad (60)$$

$$\mathcal{N} = \sum_{\sigma_{x_0}=\pm 1} \exp(-\beta H(\sigma)). \quad (61)$$

Performing the sum over σ_{x_0} leaves us with a non-linear equation:

$$\langle \sigma \rangle = \tanh(4\beta \langle \sigma \rangle). \quad (62)$$

Before we proceed with a numerical solution of the latter equation, we point out that (62) always possesses the trivial solution

$$\langle \sigma \rangle = 0.$$

A graphical inspection of (62) easily shows that for

$$\beta > \frac{1}{4}, \quad (63)$$

two non-trivial solutions $\pm c$, $c > 0$ exist. The physical interpretation of the solution is clear: for sufficiently small temperature (high β), an order phase exists. The critical value is, in mean-field approximation, given by

$$\beta_c^{\text{MF}} = 1/4. \quad (64)$$

Equation (62) can be easily solved numerically with the Newton method or by fixed point iteration. The result for the magnetisation as a function of the inverse temperature is shown in figure 2. Also shown is the exact result [2]:

$$\langle \sigma \rangle = \left[1 - \frac{1}{\sinh^4(2\beta)} \right]^{1/8} \quad (65)$$

The mean-field result qualitatively reproduces the correct phase structure. The mean field approximation is able to describe the transition from the disordered to the ordered phase. However, the mean field approximation fails at a quantitative level. The correct value for the critical value

$$\beta_c = 0.44068679\dots \quad (\text{Onsager}) \quad (66)$$

is largely underestimated. Also the rise of the magnetisation close to β_c is not correctly reproduced. A Taylor expansion of (62) with respect to β around $\beta_c^{\text{MF}} = 1/4$ (and therefore also with respect to σ), yields:

$$\langle \sigma \rangle \approx \sqrt{12} \left(\beta - \beta_c \right)^b, \quad b = \frac{1}{2}. \quad (67)$$

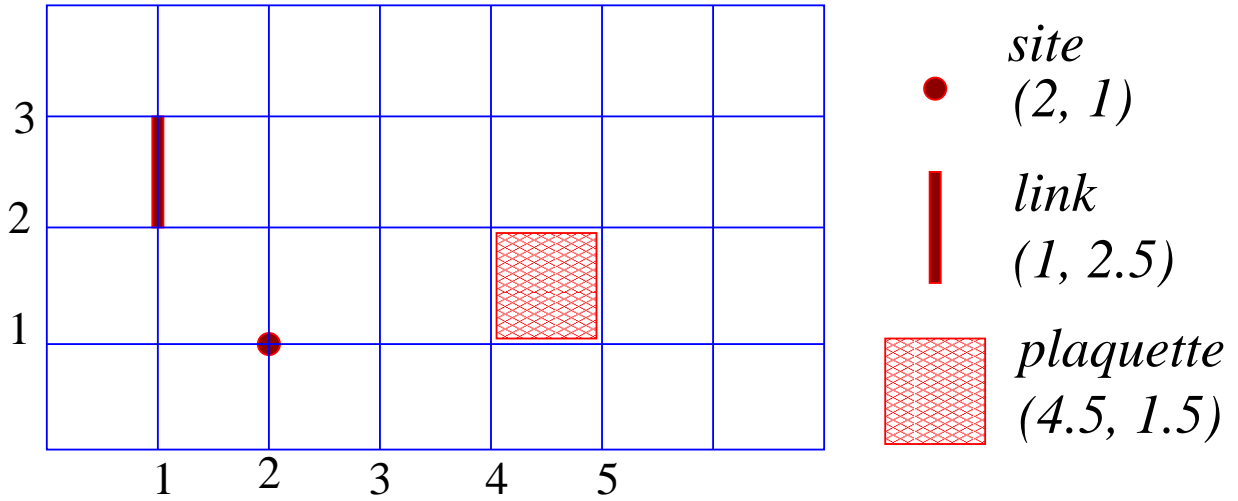


Figure 3: Geometrical objects on a lattice.

The mean field critical exponent of $1/2$ is much too large compared with the exact exponent of $b_{exact} = 1/8$.

The advantage of the mean-field approximation is that it can be easily applied to a variety of models (e.g. the Ising model in $d > 2$ where no exact results are available). It often provides a correct first impression of the phase structure. The disadvantage is that it is difficult to improve the approximation in a systematic way.

2.4 Duality transformation

Let us name different geometrical objects on a lattice. The *sites* on a lattice are labelled by integer coordinates. *Links* are short line segments which join two neighbouring sites on the lattice. In order to unambiguously address a link on the lattice, we use coordinates which are integers with the exemption of one coordinate which is half, such as 2.5 (see figure 3 for an illustration). Another important object is the so-called *plaquette*, which is an elementary square of the cubic lattice. Two coordinates are half when a plaquette is addressed. In higher dimensions, there are also *cubes*, and their coordinates are half, while the other coordinates are integer.

The *dual lattice* is an important object which helps to gain non-perturbative information for certain lattice models. The coordinates of the dual lattice are obtained by adding 0.5 to all coordinates of the lattice. If we consider a d dimensional lattice model, the duality transformation maps a x dimensional geometrical object into a $d - x$ dimensional object on the dual lattice. Let us consider 2 dimensions. A site, such as $(2, 4)$ is mapped into $(2.5, 4.5)$, which are the coordinates of a plaquette, while a link, e.g. $(1.5, 5)$, maps into another link namely $(2, 5.5)$.

With these prerequisites, let us consider the probabilistic measure of the 2d Ising model.

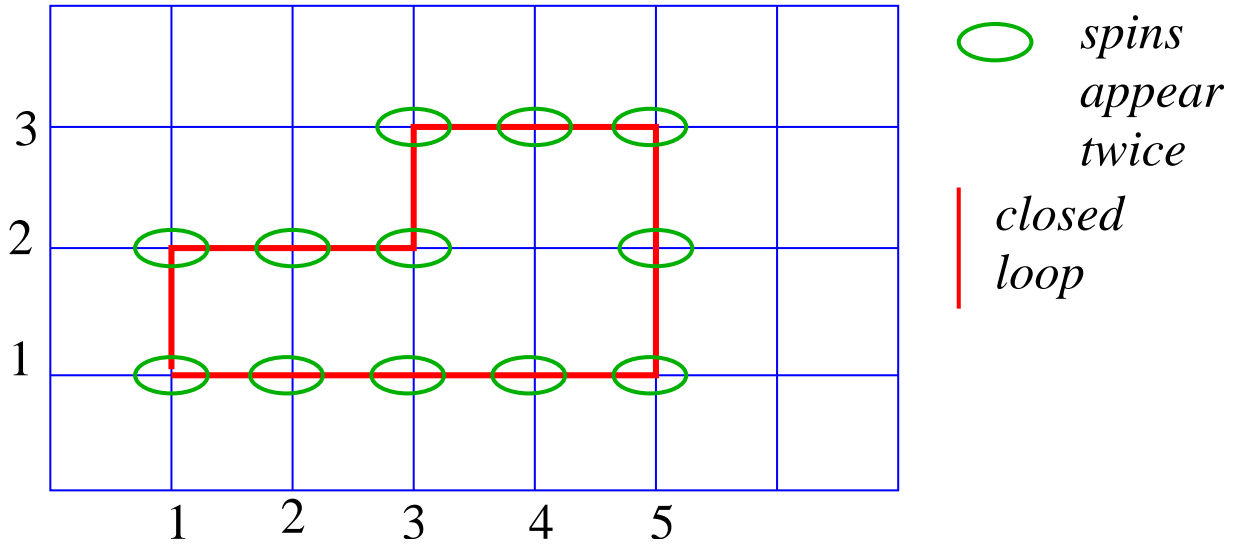


Figure 4: Integration over spins generate closed loops.

Since the product $\sigma_x\sigma_y$ can only take values ± 1 , we expand:

$$\exp\{\beta\sigma_x\sigma_y\} = a + b\sigma_x\sigma_y.$$

Inserting both possible values for the product $\sigma_x\sigma_y$, we find:

$$a + b = e^\beta, \quad a - b = e^{-\beta},$$

and finally:

$$\exp\{\beta\sigma_x\sigma_y\} = \cosh\beta + \sinh\beta\sigma_x\sigma_y. \quad (68)$$

Hence, the partition function in (56) can be written as

$$\mathcal{Z} = \sum_{\{\sigma_x\}} \cosh^{2N} \prod_{\langle xy \rangle} [1 + \tanh\beta\sigma_x\sigma_y]. \quad (69)$$

where x and y are nearest neighbours on the lattice, and the corresponding link is denoted by $\langle xy \rangle$. Note also that, in 2 dimensions, there are $2N$ links for a lattice with N sites. In order to perform the sum over all spin configurations in (69), we use the important relations:

$$\sum_{\sigma=\pm 1} \sigma = 0, \quad \sum_{\sigma=\pm 1} \sigma^2 = 2.$$

Hence, if we perform the sum over the spin σ_x in (69), we must make sure that it appears twice (or an even times) when we expand the products of the square brackets.

Thus, if we avoid a vanishing contribution to the partition function, the integration over the spins generates closed loops the corner of which the square of a particular spin appears.

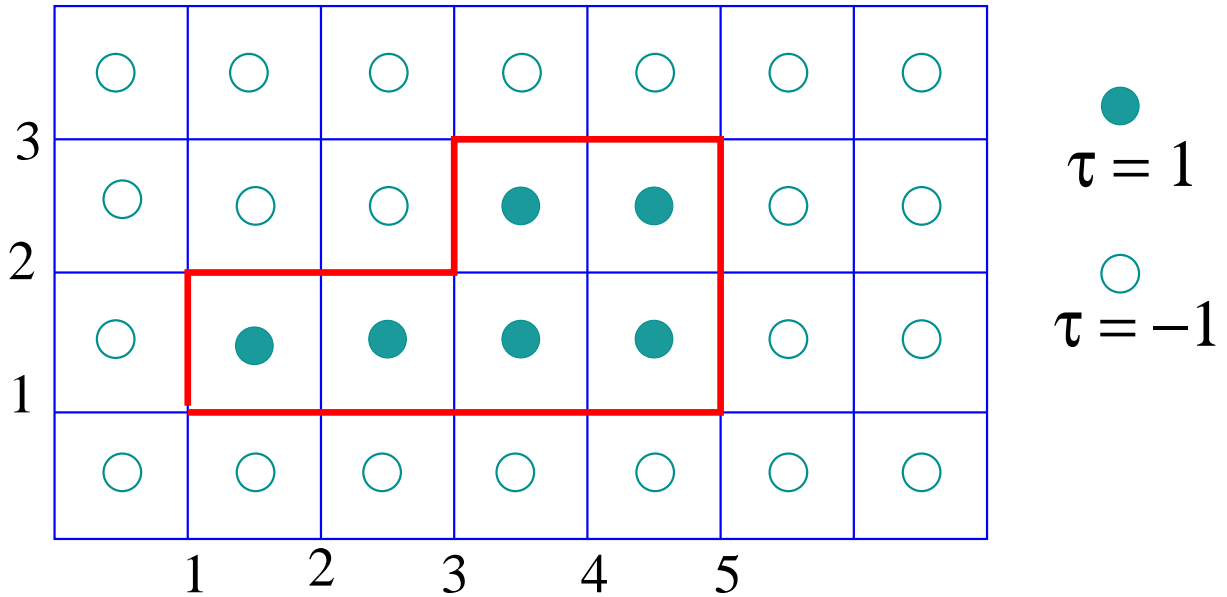


Figure 5: Introducing dual variables to represent closed loops.

For each link of the closed loop, we get a factor $\tanh \beta$. Hence, after we have integrated out all spins, the partition function can be written as:

$$\mathcal{Z} = \cosh^{2N} \beta 2^N \sum_{\text{loops}} \left[\tanh \beta \right]^{N(L)}, \quad (70)$$

where $N(L)$ is the number of links of the closed loop L . Note that we obtained a factor of 2 for each sum of the type \sum_{σ} . This gives rise to the prefactor 2^N in front of the sum in (70). We now have converted the Ising model into a string theory, but we haven't gained much information on the Ising model so far. To proceed further, we must control the sum over closed loops. For this purpose, we introduce new variables $\tau = \pm 1$ which are associated with the plaquettes (see figure 5). If we consider two neighbouring plaquettes, there is always just one link between them. Now we say that if the product of the two neighbouring plaquettes is -1 , the corresponding link is part of the loop. If the product is 1 , the link is not part of the loop. The advantage of the τ variables is that we can randomly assign ± 1 to them and all loops we are going to get are closed. Hence, summing over all possible τ configurations will do the sum over all possible closed loops for us.

Note that each plaquette of the lattice is mapped to a site on the dual lattice. The link between two neighbouring plaquettes is mapped into the link between the adjacent sites of the dual lattice. Finally, we must express $N(L)$ in terms of the τ variables. For this purpose, we have to count all *activated* links on the lattice. It is easy to check that

$$N(L) = \sum_{\langle x_d y_d \rangle} \frac{1}{2} \left[1 - \tau_{x_d} \tau_{y_d} \right] \quad (71)$$

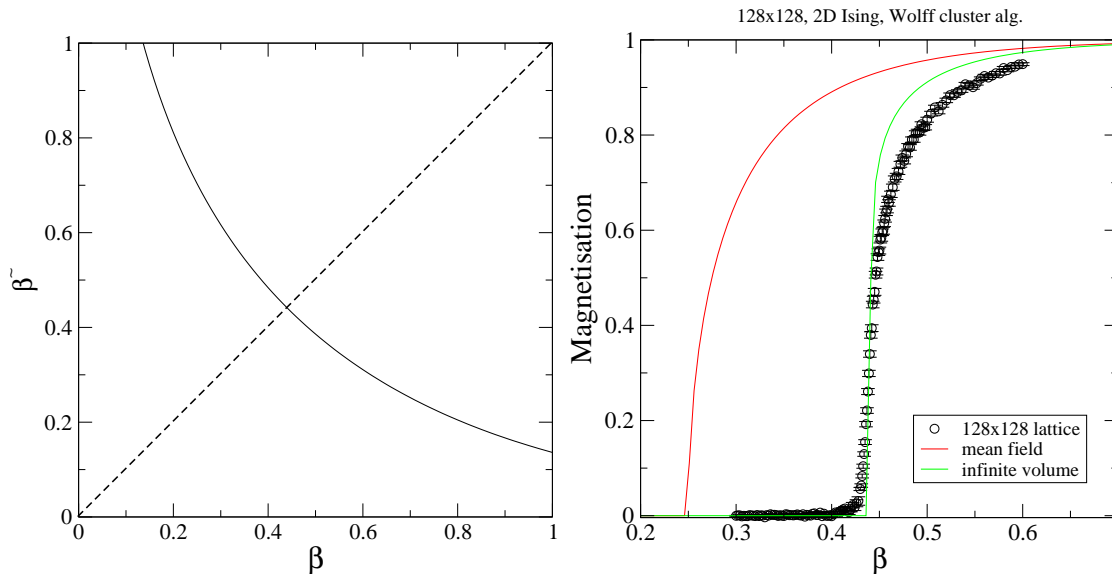


Figure 6: The dual coupling constant $\tilde{\beta}$ as a function of β (left). Magnetisation as a function of β (right).

counts these links: if two neighbouring τ s are equal, they do not contribute to $N(L)$, and if they are different, they contribute 1 as they should. Using the τ -representation of the closed loops, the partition function (70) becomes

$$\mathcal{Z} = \cosh^{2N} \beta [2 \tanh \beta]^N \sum_{\{\tau_{xd}\}} \prod_{\langle xd, yd \rangle} [\tanh \beta]^{-\frac{1}{2} \tau_{xd} \tau_{yd}}. \quad (72)$$

The latter equation can be written as

$$\mathcal{Z} = \sinh^N(2\beta) \sum_{\{\tau_{xd}\}} \exp \left\{ \sum_{\langle xd, yd \rangle} \tilde{\beta} \tau_{xd} \tau_{yd} \right\}. \quad (73)$$

$$\tilde{\beta} = -\frac{1}{2} \ln \tanh \beta. \quad (74)$$

We have obtained again a 2d Ising model which is now formulated on the dual lattice: the only difference is that the coupling is now $\tilde{\beta}$ rather than β . It is by far not generic that the duality transform yields the same lattice model just with different couplings. Models which have this property are called *self dual*.

Now let us assume that β is large (small temperature). In this case, we find from (74) that

$$\tilde{\beta} \approx e^{-2\beta}, \quad \beta \text{ large.}$$

By contrast, if β is small (the high temperature limit), we find

$$\tilde{\beta} \approx -\frac{1}{2} \ln \beta, \quad \beta \text{ small.}$$

Hence, large β corresponds to small $\tilde{\beta}$ and vice versa (see figure 6). This is interesting since the so-called *strong coupling expansion* techniques are available for small β . Doing the expansion with respect to $\tilde{\beta}$ in the dual model, also the large β regime can be studied by analytic methods. Basis of this expansion is a Taylor expansion of the exponential with respect to β . This expansion naturally reaches its radius of convergence when β approaches at the critical coupling β_c . Performing the expansion using the dual model, the Taylor expansion with respect to $\tilde{\beta}$ also breaks down at the critical coupling. There are no other couplings for which singularities in thermodynamical quantities occur. Hence, the critical point is obtained if

$$\beta = \tilde{\beta} = \beta_c. \quad (75)$$

Using (74), we therefore find

$$\beta_c = -\frac{1}{2} \ln \tanh \beta_c, \quad \beta_c = \frac{1}{2} \ln(1 + \sqrt{2}) \approx 0.44068679\dots \quad (76)$$

Figure 6 also shows the magnetisation as a function of β for a 128×128 lattice compared with the mean field result and the exact result in the infinite volume limit.

There are lot of interesting features of field theories already signalled by the Ising model: there is the conspiracy between a lattice model and string theory, and there is the duality transform which maps the high temperature theory onto a low temperature theory.

3 Markov chain Monte-Carlo: the Ising case study

3.1 Foundations

The idea central to all simulations of lattice models is to generate lattice configurations $\{\sigma_x\}$ according to their probabilistic measure

$$P(\sigma) = \exp(-\beta H(\sigma)) / \mathcal{Z} \quad (77)$$

where \mathcal{Z} is the partition function (56). A straightforward idea to accomplish this task would be to generate randomly the spins at each site x and to accept or reject this configuration according to (77). The problem is that we would hardly find any configuration which is acceptable. Why is this so?

Let us answer this question in the context of the Ising model of the previous section. The two dimensional lattice consists of $N = 125 \times 125$ sites. Since $\sigma \in \{-1, +1\}$, there are $2^N \approx 10^{4704}$ different lattice configurations. We further introduce the average action per site, i.e.

$$\bar{s} = \frac{1}{N} \left\langle \sum_{\langle xy \rangle} \sigma_x \sigma_y \right\rangle = \left\langle \mathcal{A}(x) \right\rangle =: \bar{\mathcal{A}} \quad (78)$$

where

$$\mathcal{A}(x) := \sum_{y>x, |x-y|=1} \sigma_x \sigma_y, \quad \sum_{y>x, |x-y|=1} 1 = 2. \quad (79)$$

A measure for the strength of the fluctuations of the action around its average value $N\bar{s}$ is given by

$$\delta^2 = \left\langle \left(\sum_{\langle xy \rangle} \sigma_x \sigma_y - N\bar{s} \right)^2 \right\rangle = \left\langle \left[\sum_x (\mathcal{A}(x) - \bar{\mathcal{A}}) \right]^2 \right\rangle \quad (80)$$

$$= \sum_{x,y} \langle (\mathcal{A}(x) - \bar{\mathcal{A}}) (\mathcal{A}(y) - \bar{\mathcal{A}}) \rangle . \quad (81)$$

The crucial observation is that the connected correlation function

$$D(x-y) := \langle (\mathcal{A}(x) - \bar{\mathcal{A}}) (\mathcal{A}(y) - \bar{\mathcal{A}}) \rangle \quad (82)$$

exponentially decreases for large values of $|x-y|$, i.e. $D(x) \propto \exp\{-x/\xi_A\}$, where ξ_A is the correlation length characteristic for fluctuations in the action density. Hence, one finds that its integrated strength, the so-called **susceptibility**, is finite at least for $\beta \neq \beta_c$, i.e.,

$$\rho := \sum_x D(x) < \infty . \quad (83)$$

These findings tell us that the standard deviation δ (81) linearly grows with the number of sites, i.e. $\delta = N\rho$.

Using the central limit theorem to estimate the probability distribution P_A for the action density, we find

$$P_A \approx \exp\left(-\frac{(Ns - N\bar{s})^2}{\delta^2}\right) = \left[\exp\left(-\frac{(s - \bar{s})^2}{\rho}\right) \right]^N . \quad (84)$$

Hence, in the case of many sites, only configurations with an action per site close to the average action density can significantly contribute to the partition function. If randomly choose the spins on the sites the action density can take any value between -1 and 1 , and the argument $(s - \bar{s})/\rho$ is generically of order 1. Hence the acceptance rate is down to $e^{-128 \times 128} \approx 10^{-7115}$.

The basic idea is to only generate configurations which are relevant. Starting from a seed configuration c_0 , we will generate subsequent configurations c_1, c_2, \dots . Thereby, the result for c_{i+1} should only depend on the precessing configuration c_i and must not depend on the configurations c_{i-1} . In this case, the set of configurations,

$$c_0 \longrightarrow c_1 \longrightarrow c_2 \longrightarrow c_3 \longrightarrow \dots \longrightarrow c_\infty$$

is called *Markov chain*. Central ingredient to a Markov chain is the probability $W(b, a)$ with which configuration b is created out of configuration a . This probability must satisfy certain constraints:

- (i) Normalisation $\sum_b W(b, a) = 1, \forall a$
- (ii) Ergodicity $W(b, a) > 1, \forall a, b$
- (iii) Stability $\sum_a W(b, a) P(a) = P(b), \forall b,$

where $P(a)$ is given in (77). If these conditions are met, the series c_i converges to a configuration which is distributed according to $P(c_\infty)$ (77). In order to see this, we introduce the probability $Q_i(c)$ of finding a configuration c at position i of the Markov chain, and define the deviation from the desired distribution by

$$\epsilon_i = \sum_c \left| Q_i(c) - P(c) \right|. \quad (85)$$

Because of property (ii), there is a W_{\min} with

$$W(a, b) \geq W_{\min} > 0, \quad W'(a, b) := W(a, b) - W_{\min} \geq 0. \quad (86)$$

Furthermore, the condition (i) implies that

$$\sum_c Q_i(c) = 1, \quad \sum_c P(c) = 1. \quad (87)$$

Using the stability condition (iii), we then obtain:

$$\begin{aligned} \epsilon_{i+1} &= \sum_c \left| \sum_a W(c, a) Q_i(a) - P(c) \right| = \sum_c \left| \sum_a W(c, a) [Q_i(a) - P(a)] \right| \\ &= \sum_c \left| \sum_a W'(c, a) [Q_i(a) - P(a)] + W_{\min} \sum_a [Q_i(a) - P(a)] \right| \\ &= \sum_c \left| \sum_a W'(c, a) [Q_i(a) - P(a)] \right|. \end{aligned} \quad (88)$$

Using the triangle inequality and the positivity of W' , we find

$$\epsilon_{i+1} \leq \sum_c \sum_a W'(c, a) \left| Q_i(a) - P(a) \right|. \quad (89)$$

Changing the order of summation and using (see (86))

$$\sum_c W'(c, a) = \sum_c (W(c, a) - W_{\min}) = 1 - n_{\text{conf}} W_{\min}, \quad (90)$$

where n_{conf} is the number of configurations, we finally find convergence:

$$\epsilon_{i+1} \leq [1 - n_{\text{conf}} W_{\min}] \sum_a \left| Q_i(a) - P(a) \right| = [1 - n_{\text{conf}} W_{\min}] \epsilon_i. \quad (91)$$

Instead of demanding the less stringent condition (iii), one often demands *detailed balance*:

$$(iii)' \quad W(b, a) P(a) = W(a, b) P(b) .$$

The latter condition immediately leads to condition (iii) if we sum the equation (iii)' over the configurations a :

$$\sum_a W(b, a) P(a) = \sum_a W(a, b) P(b) = P(b) ,$$

where we have used condition (i). Since condition (iii) follows from (iii)' and only (iii) is necessary for our prove above, demanding *detailed balance*, i.e., (iii)', is more restrictive.

3.2 Heat-bath algorithm

The heat-bath algorithm works as follows: (i) choose randomly a site x_0 and consider the corresponding spin $\sigma(x_0)$ for the update. Since the spin only interacts with its nearest neighbours, the interaction can be written as

$$H = \text{const.} - h_0 \sigma_{x_0} , \quad h_0 = \sum_{\langle xx_0 \rangle} \sigma_x . \quad (92)$$

The relative probability for choosing $\sigma(x_0) = 1$ is given by $\exp\{h_0\beta\}$, and the relative probability for $\sigma(x_0) = -1$ is given by $\exp\{-h_0\beta\}$. (ii) Calculate the absolute probability

$$p = \frac{\exp\{\beta h_0\}}{\exp\{-\beta h_0\} + \exp\{\beta h_0\}} \quad (93)$$

with which the spin σ_{x_0} must be set to 1. Choose a random number $z \in [0, 1]$. For $z < p$, choose $\sigma_{x_0} = 1$ and set $\sigma_{x_0} = -1$ otherwise. (iii) Subsequently, pick another spin for the update and start over with (i). Once all spins have been visited at least once, one *sweep* has been performed.

The above algorithm needs an initial configuration. We could choose a unique orientation of all spins. Since this is the ground state of the Hamiltonian which dominates the partition function for small values of the temperature, this start is called *cold start*. Alternatively, we could start with a random orientation of the spins. This is a configuration which is relevant at very high temperatures where interactions are negligible. This start is therefore called *hot start*. Independent of our choice, a number of sweeps are carried out to generate a statistical relevant configuration. This procedure is known as *thermalization*. The number which is necessary to arrive at a equilibrated spin lattice depends on the number of degrees of freedom and the temperature.

Let us now examine typical lattice spin configurations.

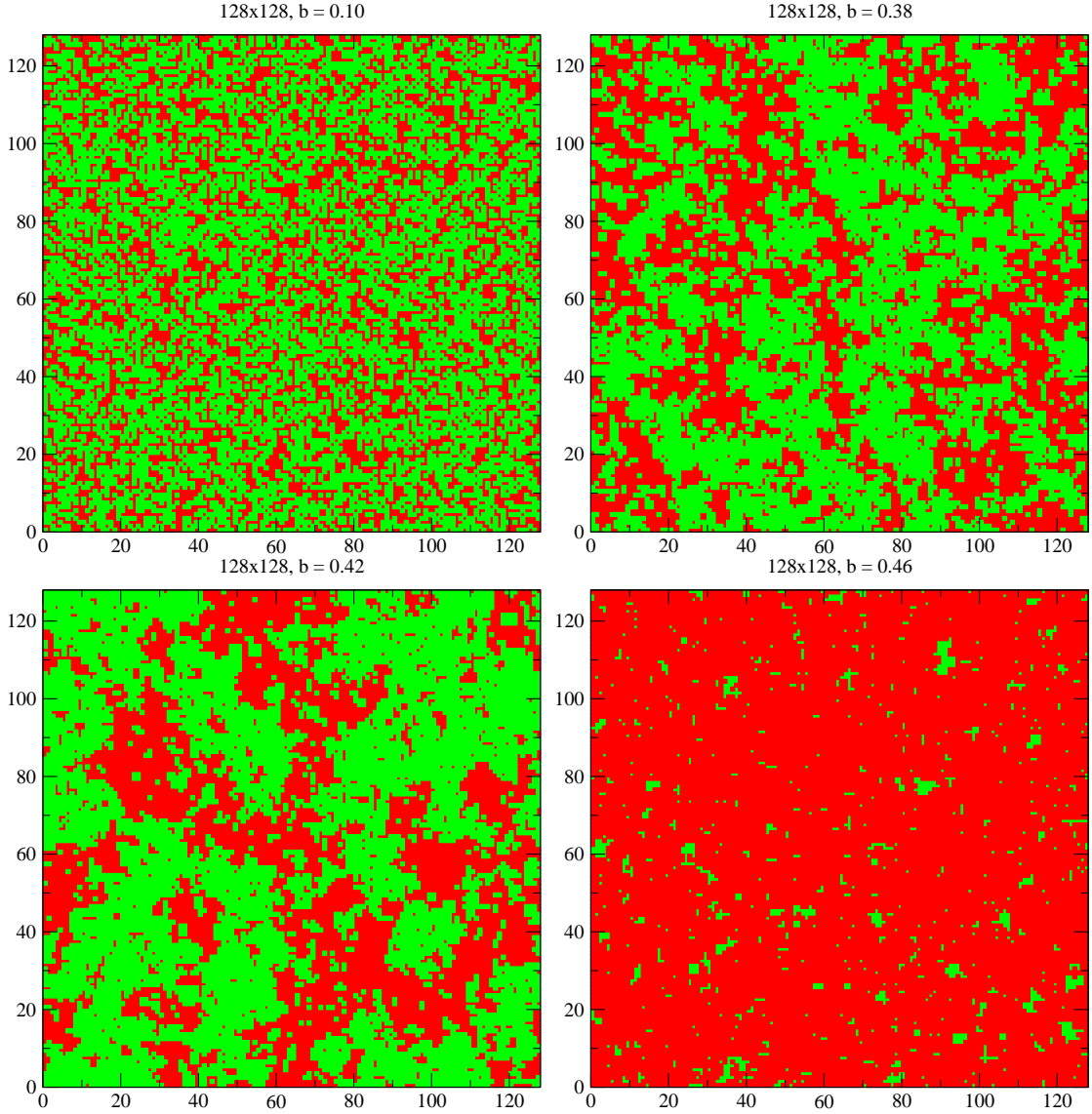


Figure 2: Thermalized spin configurations of the 2d Ising model for several β values starting from high temperature phase to the low temperature ordered phase.

Starting from low β , the sample configurations are highly disordered. Increasing β up to ≈ 0.3 , the clusters of spins with the same orientation already extend over several lattice spacings. Coming close to the critical values, e.g. for $\beta \approx 0.42$, the clusters are already as big as the lattice. This observation by eye reflects the growth of the spin correlation length which is for the present case

$$\xi \approx \xi_+ \left| 1 - \frac{T}{T_c} \right|^{-1}, \quad (T \gtrsim T_c), \quad (94)$$

which even diverges when $\beta \rightarrow \beta_c$.

In order that our numerical approach produces the configurations of a Markov chain, the configurations must not depend on the Monte-Carlo history. Whether the configurations are indeed statistical independent, we may inspect the autocorrelation time τ let's say for the magnetisation M (see subsection 1.3 for a discussions of autocorrelations). To guarantee independence, we perform of order 2τ Monte-Carlo sweeps before we consider a configuration eligible for contributing to an estimator. In the case of the heat bath algorithm (in fact, in case of all local update algorithms), one discovers that the autocorrelation time strongly increases when the critical point is approached. This implies that the interesting regime of the model, namely the regime close to the phase transition, is not accessible with these types of algorithm. The reason for this is the following: consider a spin inside one the clusters. All the neighbouring spins are pointing in the same direction. If this spin is now considered by local update procedure, the spin hardly changes because of the string mean field produced by the other spins. Hence, only the boundaries of the cluster are significantly modified after one sweeps through the lattice. The correct physics is, however, described by configurations consisting out of strongly fluctuating clusters. In order to change a cluster completely, there are roughly ξ^2 lattice sweeps necessary. Hence, only after ξ^2 sweeps, the configuration has changed significantly. This, however, implies that the autocorrelation time is roughly given by $\tau \approx \xi^2$. Indeed, it was empirically for the Metropolis algorithm that

$$\tau \approx \xi^z, \quad z_{\text{Metro}} \approx 2.125. \quad (95)$$

The index z is called *dynamical critical exponent*, and it depends on the algorithm. Since the physical correlation length ξ diverges at the phase transition, eq.(95) implies that the regime near the phase transition cannot be simulated with local update algorithms.

3.3 Cluster update algorithms

State of the art simulations which explore the transition regime make use of the so-called cluster algorithms. The difference to local update algorithms is that many spins are flipped at a time. To derive the prescription of such a cluster update, we rewrite the partition function (56)

$$\mathcal{Z} = \sum_{\{\sigma_x\}} \exp\left(\beta \sum_{\langle xy \rangle} \sigma_x \sigma_y\right) = \sum_{\{\sigma_x\}} \prod_{\langle xy \rangle} \exp(\beta \sigma_x \sigma_y). \quad (96)$$

If both neighbouring spins, σ_x and σ_y , in (96) are equal, the probabilistic factor in (96) equals $\exp \beta$. For an opposite orientation of the spins, the probabilistic factor is given by $\exp(-\beta)$. We therefore cast (96) into

$$\mathcal{Z} = \sum_{\{\sigma_x\}} \prod_{\langle xy \rangle} e^{\beta} \left[(1-p) + p \delta_{\sigma_x \sigma_y} \right], \quad p := 1 - e^{-2\beta}. \quad (97)$$

We now are going to make the representation of the partition function even more complicated by using the identity

$$a + b = \sum_{n=0}^1 \left[a \delta_{n0} + b \delta_{n1} \right].$$

Introducing the variables $n_{xy} \in \{0, 1\}$, which are associated with each link of the lattice, we obtain

$$\mathcal{Z} = \sum_{\{\sigma_x\}} \sum_{\{n_{xy}\}} \prod_{\langle xy \rangle} e^{\beta \left[(1-p) \delta_{n_{xy},0} + p \delta_{\sigma_x \sigma_y} \delta_{n_{xy},1} \right]}. \quad (98)$$

The cluster update prescription is now obtained by performing standard heat bath steps for the variables $\{\sigma_x\}$ and $\{n_{xy}\}$.

Let us consider the update for the link variables n_{xy} first. In order to avoid to generate a configuration of vanishing probability, we must choose $n_{xy} = 0$ if the neighbouring spins $\{\sigma_x\}$ and $\{\sigma_y\}$ are different (see (98)). If these spins are equally oriented, the probabilistic measure in (98) is given by

$$(1-p) \delta_{n_{xy},0} + p \delta_{n_{xy},1},$$

implying that the link n_{xy} is set to 1 with probability p . Given an initial spin distribution, the values of all link variables can be chosen according to the above prescription.

Let us now consider the spin update. According to probabilistic measure, i.e.,

$$(1-p) \delta_{n_{xy},0} + p \delta_{\sigma_x \sigma_y} \delta_{n_{xy},1},$$

all spins which are connected by links $n_{xy} = 1$ must be of equal orientation. All spins which are connected by so-called activated links are said to be part of cluster. The task is now to find all such clusters on the lattice. Once these clusters have been identified, we assign ± 1 (with equal probability) to all spins of the same cluster.

This first versions of this cluster update algorithms are due to Fortuin and Kasteleyn [3], Swendsen and Wang [4] and Wolff [5]. It is found empirically that the dynamical critical exponent is strongly reduced:

$$\tau \approx \xi^z, \quad z_{\text{cluster}} \approx 0.2. \quad (99)$$

Introductory works can be found in [3–6].

4 Quantum field theories on computers

4.1 Quantum Mechanics

Let us assume that the motion of a particle of mass m in 1 dimension is governed by a potential $V(x)$. The classical equation of motion can be calculated by variational methods

from the action

$$S = \int_0^t dt \left\{ \frac{m}{2} \dot{x}^2 - V(x) \right\}. \quad (100)$$

Classically, these equation of motion determines the time evolution of the position of the particle $x(t)$. At quantum mechanical level, the partition function

$$Z(T) = \text{Tr} \exp \left\{ -\frac{1}{T} H \right\} \quad (101)$$

is a convenient starting point to discuss the thermodynamics of the physical system. Thereby, H is the quantum mechanical Hamiltonian, i.e.,

$$H = -\frac{\hbar^2}{2m} \frac{d^2}{dx^2} + V(x), \quad (102)$$

and $\langle n|$ is the complete set of eigenstates of H . T is the temperature, and is considered as an external parameter. Once one has succeeded to calculate the partition function (101), thermodynamical quantities can be easily obtained by taking derivatives, e.g., the temperature dependence of the internal energy is given by

$$\langle H \rangle = T^2 \frac{d \ln Z(T)}{dT}. \quad (103)$$

Although a direct calculation of the eigenstates $\langle n|$ might be the easiest way to calculate a quantum mechanical partition function in practical applications, I would like to reformulate (101) in terms of a functional integral. This will be the only way to generalise the quantum mechanical considerations to the case of the quantum field theory.

For these purposes, I introduce a length scale $L := 1/T$ and an interval $[0, L]$ which I decompose into N equidistant portions of length $a \ll L$. a is called *lattice spacing*. It is trivial to obtain

$$\exp \left\{ -\frac{1}{T} H \right\} = \exp \left\{ -\sum_{\nu=1}^N a H \right\} = \prod_{\nu=1}^N \exp \{ -a H \}. \quad (104)$$

Let us define complete sets of momentum $|p\rangle$ and space $|x\rangle$ eigenstates by

$$1 = \int dx_\nu |x_\nu\rangle \langle x_\nu|, \quad 1 = \int dp_\nu |p_\nu\rangle \langle p_\nu|, \quad (105)$$

for $\nu = 1 \dots N$. As usual, these states obey

$$\langle p_k | x_k \rangle = \exp \left\{ -\frac{i}{\hbar} p_k x_k \right\}.$$

Using a complete set $|x_0\rangle$ of space eigenstates to evaluate the trace in (101), we find

$$\begin{aligned} \int dx_0 \langle x_0 | \prod_{\nu=1}^N \exp \{ -a H \} | x_0 \rangle &= \int dx_0 dp_0 dx_1 dp_1 \dots dx_{N-1} dp_{N-1} \\ &\langle x_0 | e^{-aH} | p_0 \rangle \langle p_0 | x_1 \rangle \langle x_1 | e^{-aH} | p_1 \rangle \langle p_1 | x_2 \rangle \dots \langle x_{N-1} | e^{-aH} | p_{N-1} \rangle \langle p_{N-1} | x_0 \rangle. \end{aligned}$$

Note that the operators p^2 and $V(x)$ do not commute. We may, however, write:

$$\exp \left\{ -a \frac{p^2}{2m} - aV(x) + \frac{a^2}{4m} [V(x), p^2] + \dots \right\} = \exp \{-aV(x)\} \exp \left\{ -a \frac{p^2}{2m} \right\} .$$

Since $\langle x|$ and $|p\rangle$ are eigenstates to the position operator and the momentum operator, respectively, we find

$$\langle x_k | \exp\{-aH\} | p_k \rangle = \exp \left\{ -a \left[\frac{p_k^2}{2m} + V(x_k) + \mathcal{O}(a) \right] \right\} \exp \left\{ \frac{i}{\hbar} p_k x_k \right\} .$$

The partition function therefore becomes up to terms of order a^2

$$\begin{aligned} Z(T) &= \int dx_0 dp_0 dx_1 dp_1 \dots dx_{N-1} dp_{N-1} dx_N \exp \left\{ -a \sum_{k=0}^{N-1} \left[\frac{p_k^2}{2m} + V(x_k) \right] \right\} \\ &\quad \exp \left\{ -\frac{i}{\hbar} \sum_{k=0}^{N-1} p_k (x_{k+1} - x_k) \right\} \langle x_0 | x_N \rangle \end{aligned} \quad (106)$$

It is straightforward to perform the momentum integrations, which are Gaussian, i.e.

$$\begin{aligned} Z(T) &= \left(\frac{4\pi m}{a} \right)^{N/2} \int dx_0 dx_1 \dots dx_N \delta_{x_0 x_N} \\ &\quad \exp \left\{ -a \sum_{k=0}^{N-1} \left[\frac{m}{2} \frac{(x_{k+1} - x_k)^2}{a^2 \hbar^2} + V(x_k) \right] \right\} \end{aligned} \quad (107)$$

The latter equation is a completely regularised expression for the partition function. This version can be directly used in numerical simulations. Note that in the framework of quantum field theory units are chosen in such a way that $\hbar = 1$ holds.

A compact notation can be derived by formally taking the lattice spacing a to zero. For this purpose, we define $a_h := \hbar a$, and the Euclidean action by

$$S_E = \int_0^L d\tau \left\{ \frac{m}{2} \dot{x}^2 + V(x) \right\} . \quad (108)$$

Note the sign change in front of the potential compared with the standard action (100). The interval $[0, L]$, which was introduced above (104), is called *Euclidean time* interval. By construction (see above), the length of the Euclidean time interval is given by the inverse temperature, i.e., $L = 1/T$. We also introduce an Euclidean particle trajectory, and an Euclidean velocity

$$x_k \rightarrow x(\tau) \quad \frac{x_{k+1} - x_k}{a_h} \rightarrow \dot{x}(\tau) , \quad (109)$$

where we identify $d\tau = a_h$. Using the shorthand notation

$$\left(\frac{4\pi \hbar m}{a_h} \right)^{N/2} \int dx_0 dx_1 \dots dx_{N-1} \rightarrow \mathcal{D}x(\tau) ,$$

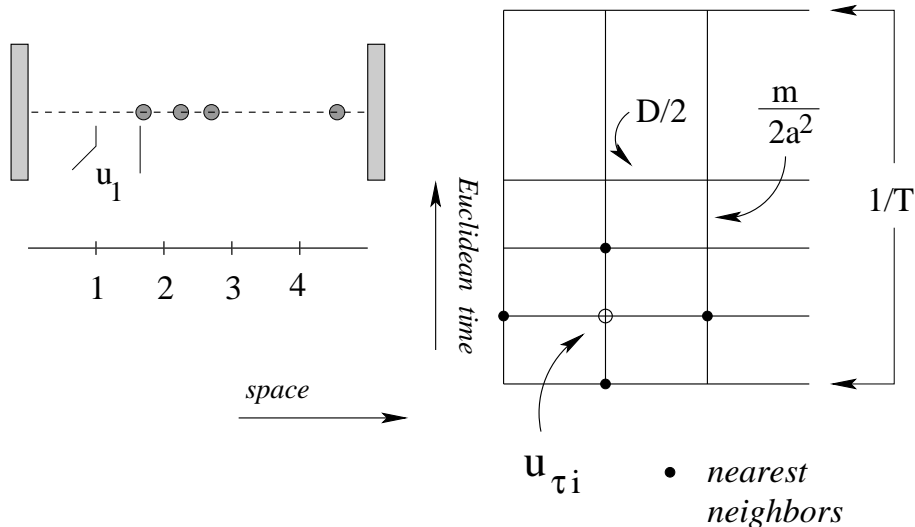


Figure 7: Classical versus quantum partition function of a 1-dimensional particle chain.

the partition function (107) can be formally written as a functional integral

$$Z(T) = \int \mathcal{D}x(\tau) \exp\left\{-\frac{1}{\hbar} S_E\right\}. \quad (110)$$

Eq.(110) suggests that an average over all Euclidean trajectories $x(\tau)$ must be performed where the probabilistic weight of each trajectory is given by $\exp\{-S_E\}$. Note also that in view of the δ -function in (107) only trajectories which are periodic in Euclidean time must be considered, i.e., $x(0) = x(L = 1/T)$.

4.2 Quantum field theory

For illustration purposes, we consider the 1-dimensional particle chain in figure 7. Thereby, the position of the particles $i = 0 \dots n$ are characterised by their elongation u_i from the equilibrium position. The particles experience a harmonic potential depending on the distance to the nearest neighbour. Here, I choose the boundary conditions $u_0 = 0$, $u_n = 0$. The Hamilton-function, which describes the classical physics, is given by

$$\mathcal{H} = \sum_{i=1}^{n-1} \left[\frac{1}{2m} p_i^2 + \frac{D}{2} (u_{i+1} - u_i)^2 \right]. \quad (111)$$

Hence the classical partition function is given by the high-dimensional integral

$$Z_{cla}(T) \propto \int dp_1 \dots dp_{n-1} du_1 \dots du_{n-1} \exp\left\{-\frac{\mathcal{H}}{T}\right\}. \quad (112)$$

In order to calculate the full quantum mechanical partition function of the particle chain, we firstly write down the Euclidean partition function. Note for this purpose that the

displacements u_i now acquire an additional dependence on the Euclidean time $u_i \rightarrow u_i(\tau) \equiv u_{\tau i}$. With this notation the Euclidean action is given by

$$S_E = \sum_{\tau=1}^N \sum_{i=1}^{n-1} a \left[\frac{m}{2a^2} (u_{\tau i} - u_{\tau-1 i})^2 + \frac{D}{2} (u_{\tau i+1} - u_{\tau i})^2 \right]. \quad (113)$$

The interactions between the c-number fields $u_{\tau i}$ can be easily visualised (see figure 7): the fields $u_{\tau i}$ harmonically interact with their nearest neighbours. The harmonic interaction strength is given by $D/2$ in space direction and $m/2a^2$ for neighbours in Euclidean time direction. The quantum mechanical partition function can be calculated by integrating over of the fields $u_{\tau i}$ located at the sites of a 2-dimensional grid, .i.e.

$$Z(T) \propto \int \mathcal{D}u \exp\{-S_E\}, \quad (114)$$

where the temperature enters the consideration via the extension of the lattice in Euclidean time direction with fields obeying periodic boundary conditions.

To conclude, we observe that the classical partition function of a $D + 1$ dimensional field theory (in lattice regularisation) corresponds to the partition function of a D dimensional quantum system. D is the number of space dimensions. This correspondence is very helpful in understanding the quantum behaviour of a theory, since it can be mapped to a classical field theory (at the expense of an additional dimension). In the next section, we will study the classical partition functions in the 4-dimensional Euclidean space in order to derive the information on the thermodynamics of the full quantum system

5 Lattice gauge theory

5.1 The gauged Ising model

The Ising model, strictly speaking the partition function (56), is invariant under the *global* transformation of the spins according to

$$\sigma^\Omega(x) = \Omega \sigma(x), \quad \Omega = \pm 1. \quad (115)$$

The transformation is called *global* because the transformation affects all spins at the same time, .i.e., Ω is independent of the coordinates. The corresponding symmetry group is Z_2 .

This symmetry group can be upgraded to a *local* symmetry, also known as *gauge symmetry*, by demanding invariance under

$$\sigma^\Omega(x) = \Omega(x) \sigma(x), \quad \Omega(x) = \pm 1. \quad (116)$$

Of course, the action (57) of the standard Ising model is not invariant under the huge symmetry group which is now $[Z_2]^N$, where N is the number of sites. In order to obtain

a version of the Ising model which possesses a Z_2 gauge symmetry, we need to change the action. The only way to do it, is to introduce an additional field, here $Z_\mu(x)$. This field is associated with the links of the lattice: x specifies the site and μ the direction in which we find the link. Alternatively, we could write:

$$Z_\mu(x) = Z_{\langle xy \rangle}, \quad y = x + \hat{e}_\mu,$$

where \hat{e}_μ is the unit vector in μ direction. For the latter expression, we will also write in short:

$$x + \hat{e}_\mu = x + \mu.$$

For the action, we choose

$$S_{\text{matter}} = \kappa \sum_{\langle xy \rangle} \sigma(x) Z_\mu(x) \sigma(x + \mu), \quad (117)$$

and demand that the link Z_μ transforms under gauge transformations as

$$Z_\mu^\Omega(x) = \Omega(x) Z_\mu(x) \Omega(x + \mu). \quad (118)$$

Since spin and link transform simultaneously with the same $\Omega(x)$ and since $\Omega^2(x) = 1$, one easily proves gauge invariance of the action (117).

Obviously, the action S_{matter} describes the interaction between the *matter* fields, i.e., the spins, and the new link fields. What is left to do, is to design a gauge invariant action for these new degrees of freedom. This interaction should be short ranged in order to preserve some very good field theoretical features (universality). A possible choice is

$$S_{\text{link}} = \beta \sum_{x, \mu > \nu} P_{\mu\nu}(x), \quad P_{\mu\nu}(x) = Z_\mu(x) Z_\nu(x + \mu) Z_\mu(x + \nu) Z_\nu(x). \quad (119)$$

Thereby, the numbers $(x, \mu > \nu)$ specify the plaquette of the lattice, the left lower corner is located at site x and which is spanned by the directions μ and ν . The field combination $P_{\mu\nu}(x)$ is often called in short the plaquette. The proof that $P_{\mu\nu}(x)$ is invariant under gauge transformations (118) is left to the reader.

The total action of the gauged Ising model has two parts: the matter part and the “gauge” part. Correspondingly, there are two coupling constants: the convention is that β is the pre-factor in the pure gauge action, while κ multiplies the matter part.

Once our system is now gauged, it only makes sense to consider gauge invariant observables since non-gauge invariant quantities vanish. Let us explore this for a simple gauge variant quantity such as the spin correlation function:

$$C(x_0, y_0) = \frac{1}{\mathcal{Z}} \sum_{\{\sigma\}} \sigma(x_0) \sigma(y_0) \exp \left\{ S[\sigma] \right\}, \quad S[\sigma] = S_{\text{matter}} + S_{\text{link}}, \quad (120)$$

$$\mathcal{Z} = \sum_{\{\sigma\}} \exp \left\{ S[\sigma] \right\}, \quad (121)$$

Let us now consider a particular gauge transformation (116) of the spins, i.e.,

$$\Omega(x) = \begin{cases} -1 & \text{for } x = x_0 \\ 1 & \text{else} \end{cases} \quad (122)$$

Renaming all spins in the sum in (120) by $\sigma(x) \rightarrow \sigma^\Omega(x)$, we use the gauge invariance of the action and the sum, i.e.,

$$S[\sigma] = S[\sigma^\Omega], \quad \sum_{\{\sigma\}} = \sum_{\{\sigma^\Omega\}}.$$

The sum is trivially invariant, since we sum anyhow over all possible ± 1 combinations for the spins. Thus, we obtain:

$$\begin{aligned} C(x_0, y_0) &= \frac{1}{\mathcal{Z}} \sum_{\{\sigma\}} \sigma^\Omega(x_0) \sigma^\Omega(y_0) \exp \{S[\sigma]\} \\ &= \sum_{\{\sigma\}} [-\sigma(x_0)] \sigma(y_0) \exp \{S[\sigma]\} = -C(x_0, y_0), \end{aligned} \quad (123)$$

where we used our particular choice (122) in the last line above. We conclude from this that $C(x_0, y_0) = 0$.

Let us now consider the particular case $\kappa = 0$ when the matter fields are absent from the theory. The emerging theory is called *pure* Z_2 gauge theory, and it is a theory of link fields only. What are the physical (i.e. gauge invariant) degrees of freedom in this case? Let us consider the more interesting case of 3 dimensions for these considerations. In order to talk about gauge invariant information, we now consider the plaquettes P_p , $p = (x; \mu\nu)$ (119). We say that a short flux line (vortex) possesses through the plaquette p if $P_p = -1$. Since the plaquette variables P are gauge invariant, so the flux lines are. More formally, we could introduce a vortex plaquette variable by:

$$v_p = \prod_{l \in p} Z_l. \quad (124)$$

Let us now consider the flux lines which enter/leave an elementary cube of the lattice. We take the product of all vortex plaquettes which are associated with the faces of the elementary cube and find:

$$\prod_{p \in c} v_p = (-1)^\nu, \quad (125)$$

where ν is the total number of vortices at the faces of the cube. Inserting the definition, we also find that

$$\prod_{p \in c} v_p = \prod_{p \in c} \prod_{l \in p} Z_l = 1, \quad (126)$$

since in the latter products all Z_l factors appear twice (see figure 8, left panel; remember $Z_l^2 = 1$). Comparing (126) with (125), we realise that ν must be even. In particular, $\nu = 1$ is excluded implying that a vortex never ends inside a cube. Hence, we find that the gauge invariant vortices form closed lines in space. See figure 8, right panel, for an illustration.

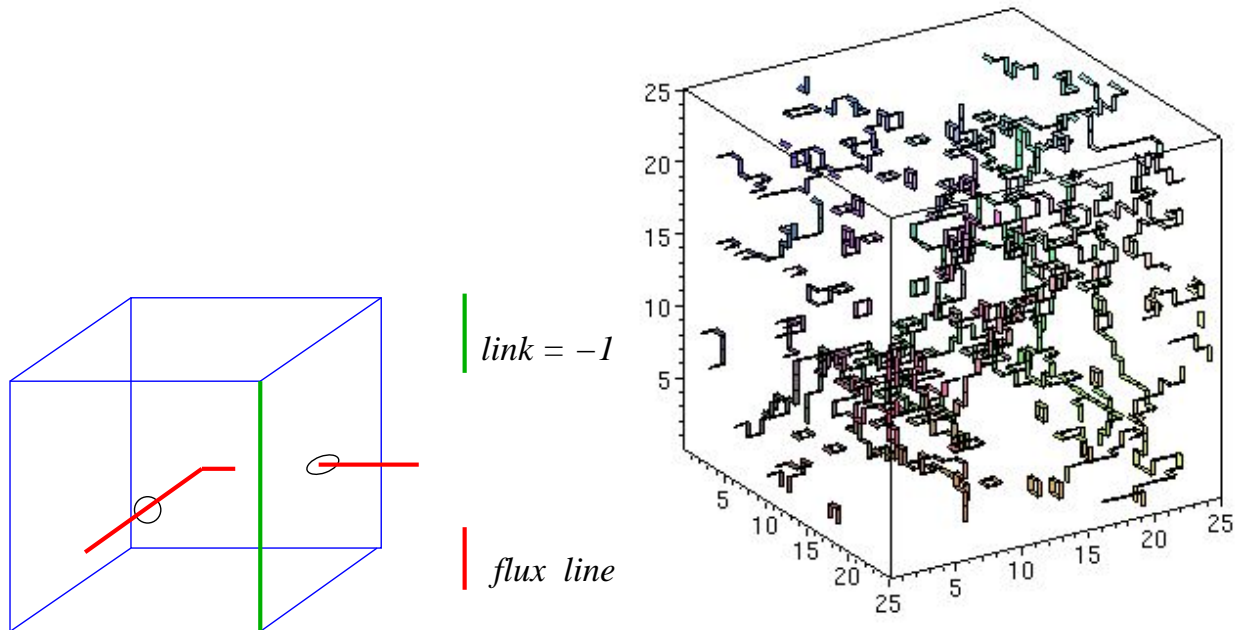


Figure 8: Flux entering an elementary cube (left) and closed flux lines on a 3d lattice (right).

5.2 Setting up lattice Yang-Mills theory

Due to the universality conjecture, the construction of lattice model with the correct number of dimensions and the correct symmetries is sufficient to simulate a uniquely defined quantum field theory in the critical limit of the lattice model. The purpose of the present subsection is to propose a classical lattice model which satisfies this prerequisite in the case of Yang-Mills theory.

It turns that in view of the large symmetry group of Yang-Mills theory choosing a classical lattice model which recovers this large symmetry group in the critical limit is cumbersome. In the case of Yang-Mills theory, the matter fields (e.g. quarks) belong to the fundamental representation of the so-called $SU(N_c)$ colour group. **Gauge invariance** means that the action of the quarks fields is invariant under *local* unitary transformations, i.e.,

$$q(x) \rightarrow q'(x) = \Omega(x) q(x), \quad \Omega(x) \in SU(N_c). \quad (127)$$

As it is explained in many text books, an invariance of the quark kinetic term is only achieved by introducing additional dynamical fields, i.e., the gluon fields $A_\mu(x)$.

The quark fields are associated with the sites in a lattice formulation. Hence, the symmetry group of the classical lattice Yang-Mills model is $[SU(N_c)]^{N_s}$, where N_s is the number of lattice sites. In order to install such a high symmetry in the critical limit of a lattice model, it has turned out fruitful to realize the symmetry even for finite values of the lattice spacing

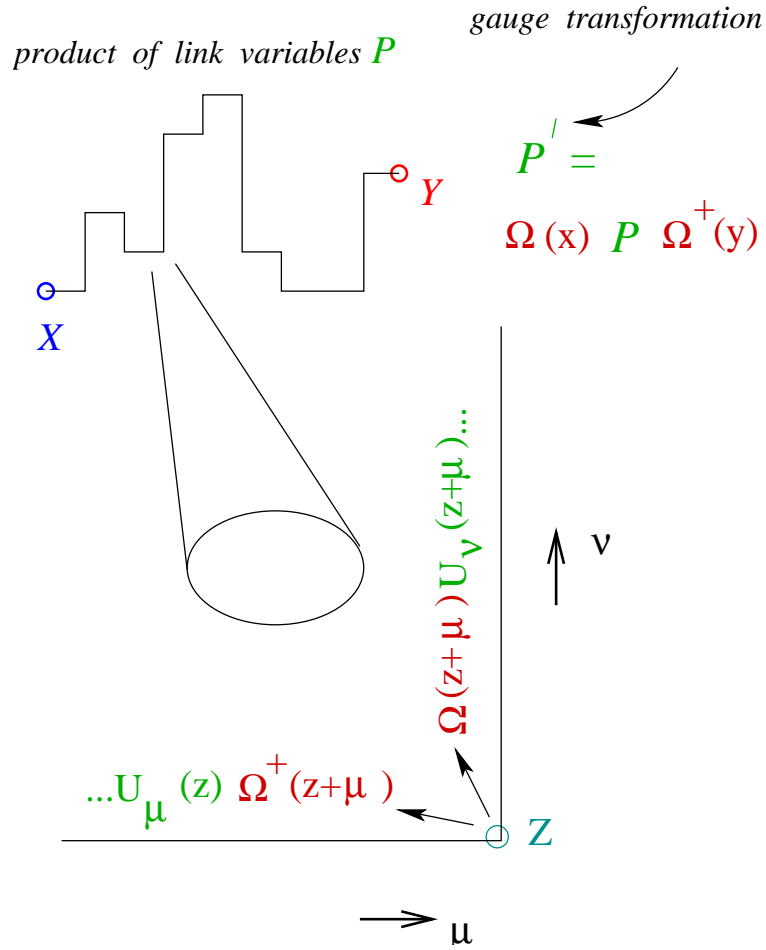


Figure 9: Path ordered product of link variables.

a. This in turn forces the model to attain gauge invariance in the continuum limit [7]. A potential candidate for a quark kinetic term is for the non-interacting case

$$\sum_{x,\mu} \frac{1}{2} \left[\bar{q}(x) \gamma_\mu q(x + \mu) - \bar{q}(x + \mu) \gamma_\mu q(x) \right], \quad (128)$$

where γ_μ are the Euclidean γ matrices. Of course, the latter equation is not invariant under the gauge transformations (127). In order to install this invariance, we introduce an additional field which is of vector type, i.e., which is related to the links of the lattice:

$$U_\mu(x) \in SU(N_c). \quad (129)$$

Generalising the quark kinetic term (128) to

$$S_Q = \sum_{x,\mu} \frac{1}{2} \left[\bar{q}(x) \gamma_\mu U_\mu(x) q(x + \mu) - \bar{q}(x + \mu) \gamma_\mu U_\mu^\dagger(x) q(x) \right], \quad (130)$$

$$P_{\mu\nu}(\mathbf{x}) = \frac{1}{N_c} \text{tr} \left[\text{square with path} \right]$$

Figure 10: Lattice plaquette variable

one observes the desired local invariance if one demands that the link fields transform as

$$U_\mu(x) \rightarrow \Omega(x) U_\mu(x) \Omega^\dagger(x + \mu) . \quad (131)$$

As in the case of continuum Yang-Mills theory, we would like to equip the lattice model with an kinetic term for the additional fields $U_\mu(x)$. For lattice models, “kinetic” means that interaction of the fields on the lattice is *short range*, i.e., that it involves only the nearest neighbours. In order to design such a kinetic term in a gauge invariant way for every value of the lattice spacing, we firstly investigate the transformation properties of a path ordered product of link variables along an open path C which starts at point x and ends at y (see figure 9 for an illustration),

$$P(x, y) = \prod_{x \in C} P U(x) . \quad (132)$$

Inserting the gauge transformed links (131) into (132), one finds

$$P(x, y) \rightarrow P'(x, y) = \Omega(x) P(x, y) \Omega(y) . \quad (133)$$

With the help of (132), it is easy to construct a kinetic term for the link variables which (i) is gauge invariant and (ii) only involves next to nearest neighbours. For this purpose, one chooses C to be a closed path starting at x and ending at $y = x$ which encircles an elementary **plaquette** (see figure 10):

$$\begin{aligned} P_{\mu\nu}(x) &= \frac{1}{N_c} \text{tr} P(x, y) \\ &= \frac{1}{N_c} \text{tr} \left\{ U_\mu(x) U_\nu(x + \mu) U_\mu^\dagger(x + \nu) U_\nu^\dagger(x) \right\} . \end{aligned} \quad (134)$$

Using (133) and the invariance of the trace under cyclic permutations, one easily shows that the plaquette (134) is gauge invariant.

The lattice partition function involves an integration over the dynamical fields of the theory. In the case of the link variables, the question arises which measure $\mathcal{D}U_\mu$ applies for the integrations. In order to preserve gauge invariance, we demand that the integration over the matrix $U_\mu(x)$ is equipped with the so-called Haar measure which satisfies

$$dU_\mu(x) = d\left(AU_\mu(x)B\right), \quad A, B \in SU(N_c). \quad (135)$$

The Haar measure is available in closed form for the unitary groups $SU(N_c)$. Here, I will present the Haar measure for a $SU(2)$ group integration where the $SU(2)$ unitary matrix U is parameterised with the help of Pauli matrices

$$U = a_0 + i\vec{a}\vec{\tau}, \quad UU^\dagger = 1 \rightarrow a_0^2 + \vec{a}^2 = 1. \quad (136)$$

Since the constraint $UU^\dagger = 1$, i.e. $a_0^2 + \vec{a}^2 = 1$, is not changed if U is multiplied with A from the left and B from the right, respectively, these multiplications can be viewed as rotations in the 4-dimensional space spanned by (a_0, \vec{a}) . Therefore, an invariant measure can be defined by

$$dU = da_0 da_1 da_2 da_3 \delta\left(a_0^2 + \vec{a}^2 - 1\right). \quad (137)$$

Introducing polar coordinates for the 3-dimensional vector $\vec{a} := a\vec{n}$, $\vec{n}\vec{n} = 1$, the integration over the length a can be performed with the help of the δ function in (137). We obtain the final result for the $SU(2)$ Haar measure, i.e.,

$$dU = da_0 \sqrt{1 - a_0^2} d\Omega_{\vec{n}}, \quad (138)$$

which is commonly used in lattice simulations.

Finally, the lattice representation of the gauge invariant partition function is given by

$$Z(T, V) = \int \mathcal{D}U \mathcal{D}q \mathcal{D}q^\dagger \exp\left\{-S_Q + \beta \sum_{x, \mu > \nu} \frac{1}{2} [P_{\mu\nu}(x) + \text{h.c.}]\right\}, \quad (139)$$

where the quark interaction is encoded in S_Q (130) and $P_{\mu\nu}(x)$ is the plaquette (134). β is related to the bare gauge coupling constant g of the continuum formulation by $\beta = 2N_c/g^2$. The particular choice of lattice regularised gluonic action is known as *Wilson action* [7]. Note that the fields $q(x)$, $q^\dagger(x)$ are anti-commuting Grassmann fields. This choice for the fermionic fields is necessary to obtain the correct Fermi statistics as well as to ensure the Pauli principle. It implies that the lattice model (139) can not be straightforwardly be used in numerical simulations. However, since the action for the quark fields is quadratic, the integration over the quark fields can be performed analytically:

$$\int \mathcal{D}q \mathcal{D}q^\dagger \exp\left\{-\bar{q}_A M_{AB} q_B\right\} = \text{Det}M[U]. \quad (140)$$

where the index A comprises space-time as well as spinorial, etc. indices. The quark determinant $\text{Det}M[U]$ is a gauge invariant function of the link variables $U_\mu(x)$. Note however that link interaction mediated by the quark determinant is non-local, implying that a link at a particular site is coupled to all other links of the lattice. In practice, this implies that a local update of a single link enforces the calculation of a functional determinant. This explains why the numerical simulation of Yang-Mills theory with dynamical quarks needs much more computational resources than the simulation of the theory in **quenched approximation**, where the quark determinant is neglected for the update of the link variables.

5.3 The fermion doubling problem

It turns out that the treatment of the quark degrees of freedom in (139) is still too naive: since the Dirac equation is linear in the momentum, its lattice analogue does not only produce the desired quark degree of freedom in the limit $a \rightarrow 0$, but 2^D (D is the number of space time dimensions) fermion flavours emerge. This observation can be already anticipated in the free theory case.

Let us firstly introduce the generating functional for connected Green's functions for the case of free and massless bosonic theory

$$Z[j] = \int \mathcal{D}\phi \exp \left\{ -\frac{1}{2} \phi_k \Pi_{kl} \phi_l + j_x \phi_x \right\}. \quad (141)$$

A sum is understood over indices which appear twice. One easily verifies that the connected correlation function is obtained from $Z[j]$ via

$$f(x-z) := \langle \phi_x \phi_z \rangle - \langle \phi_x \rangle \langle \phi_z \rangle = \frac{d \ln Z[j]}{dj_x dj_z}. \quad (142)$$

By "completing the square" in (141), we find

$$Z[j] \propto \exp \left\{ \frac{1}{2} j_x \left(\Pi^{-1} \right)_{xz} j_z \right\}, \quad (143)$$

and hence for the free bosonic case

$$\langle \phi_x \phi_z \rangle - \langle \phi_x \rangle \langle \phi_z \rangle = \left(\Pi^{-1} \right)_{xz}. \quad (144)$$

In order to evaluate the inverse of the "kinetic" term Π^{-1} , we introduce its eigenvalues and eigenvectors, i.e.,

$$\Pi |k\rangle = \lambda_k |k\rangle, \quad (145)$$

and formally write

$$\left(\Pi^{-1} \right)_{xz} = \sum_k |k\rangle \frac{1}{\lambda_k} \langle k|. \quad (146)$$

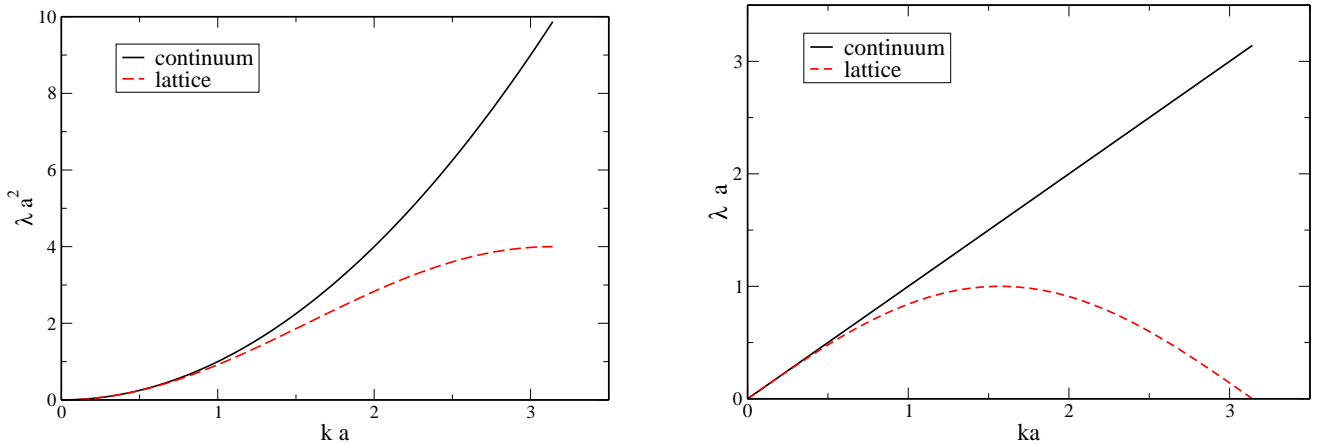


Figure 11: Dispersion relation for the tree level kinetic (continuum versus lattice formulation) for the bosonic case (left) and the fermionic case (right panel).

It is now easy to calculate the correlation function for the continuum case $\Pi = -\partial^2$. The eigenfunctions are subjected to periodic boundary conditions $\phi(x) = \phi(x + L)$, i.e.,

$$\phi(x) \propto e^{ikx}, \quad e^{ikL} = 1, \quad k = \frac{2\pi}{L}n, \quad n \in Z. \quad (147)$$

The discrete k levels are called **Matsubara frequencies**. In the continuum, there is no further restriction on the integer n . Making the ansatz (147), we find that the eigenvalues are given by

$$\lambda(k) = k^2 \quad (\text{continuum}). \quad (148)$$

Hence, a free massless particle manifests itself in the correlation function (146) as pole at zero momentum transfer. In the case of the lattice theory, the lattice version of the eigenvalue equation is

$$\Pi\phi(x) = \sum_{\mu} \left[-\phi(x + \mu) + 2\phi(x) - \phi(x - \mu) \right] = \lambda_{\text{latt}} a^2 \phi(x). \quad (149)$$

In order to solve this equation, we use the plane wave ansatz (147). One crucial difference between the lattice and the continuum version is that only wavelengths l obeying

$$\frac{l}{2} \geq a, \quad \frac{\pi}{k} \geq a \quad (150)$$

are sensible. The lattice naturally provides an UV momentum cutoff, i.e., $\Lambda_{UV} = \pi/a$. Inserting (147) into (149) one finds

$$\lambda_{\text{latt}} a^2 = \sum_{\mu} \left[2 - e^{ik_{\mu} a} - e^{-ik_{\mu} a} \right] = 4 \sum_{\mu} \sin^2 \left(\frac{k_{\mu} a}{2} \right). \quad (151)$$

For momenta which are small compared to the UV cutoff, i.e., $ka \ll \pi$, we recover the continuum dispersion relation

$$\lambda_{latt} = k^2 \left[1 + \mathcal{O}(k^2 a^2) \right]. \quad (152)$$

In figure 11 the dispersion relation of the continuum formulation is compared to the one of the lattice version. Also in the lattice case, the correlation function only shows one singularity reflecting that in the scaling limit $\lambda a^2 \ll 1$, $ka \ll \pi$, the dispersion relation of one free particle is recovered.

Let us study the fermionic case. In order to reproduce the correct Fermi statistics, fermion fields $\psi(x)$ are of Grassmann type and obey anti-periodic boundary conditions. I refer to the textbooks [1] for an introduction into a free fermionic theory, and only quote the final result for the correlation function which formally agrees with (146). In the continuum, the eigenvalue equation is given by

$$\Pi\psi(x) = \not{\partial}\psi(x) = \lambda\psi(x), \quad (153)$$

where anti-hermitian (Euclidean) γ matrices are used. The ansatz for the spinor wave functions is again of plane wave type, i.e.,

$$\psi(x) \propto u(k) e^{ikx}, \quad e^{ikL} = -1, \quad k = \frac{2\pi}{L} \left(n + \frac{1}{2} \right), \quad n \in Z. \quad (154)$$

The spectrum $\lambda(k)$ is determined by making the ansatz

$$u(k) = \left[i\not{k} + \lambda \right] u_0, \quad (155)$$

which yields

$$\left[i\not{k} - \lambda \right] u(k) = \left[i\not{k} - \lambda \right] \left[i\not{k} + \lambda \right] u_0 = 0, \quad (156)$$

and therefore

$$\left[k^2 - \lambda^2 \right] u_0 = 0. \quad (157)$$

Hence, the spectrum of the continuum theory is linearly increasing: $\lambda = \sqrt{k^2}$. Using the kinetic energy for a free quark theory introduced in (128), the lattice version of the eigenvalue equation is given by

$$\frac{1}{2} \sum_{\mu} \left[\gamma_{\mu} \psi(x + \mu) - \gamma_{\mu} \psi(x - \mu) \right] = \lambda a \psi(x). \quad (158)$$

The ansatz (154) also provides the eigenvectors to the eigenvalues problem (158). Repeating the steps which have led to the continuum dispersion relation, one finds in the lattice case

$$\lambda a = \sqrt{\sum_{\mu} \sin^2(k_{\mu} a)}. \quad (159)$$

The fermionic eigenvalue distribution is also shown in figure (11). Close to the critical limit when $\lambda a \ll 1$ holds, one recovers the continuum dispersion relation from (159) by making a Taylor expansion with respect to ka . In addition, a second singularity occurs for $ka \approx \pi$. This shows that even in the case that $\lambda a \ll 1$ a second fermion flavour arises from lattice fermion action (128).

It can be shown that this fermion doubling problem necessarily occurs for a chiral invariant action which is translation invariant and local (Nielsen-Ninomiya No-Go theorem). At the present stage, a lot of research effort is devoted to incorporate chiral symmetry at the expense of a moderate non-locality of the action [8].

5.4 Overlap Fermions

In the continuum formulation, the chiral invariant Dirac operator \mathcal{D} satisfies the relations

$$\{\mathcal{D}, \gamma_5\} = 0, \quad \{\mathcal{D}^{-1}, \gamma_5\} = 0, \quad (160)$$

which tells us that the non-zero eigenvalues $\bar{\lambda}$ appear in pairs $\{\bar{\lambda}, -\bar{\lambda}\}$. Let D denote a lattice candidate of the Dirac operator (in units of the lattice spacing a) which satisfied the so-called *Ginsparg-Wilson relation* [9]

$$\{D, \gamma_5\} = 2D\gamma_5D. \quad (161)$$

One observes that the right hand side of (161) is of order $\mathcal{O}(a^2)$ (compared with the order $\mathcal{O}(a)$ of the left hand side) implying that the naive continuum limit $a \rightarrow 0$ of (161) reduces to the chiral relation (160). The most important observation is however that a certain remanent of the chiral symmetry is present in the lattice version. Defining

$$\tilde{D}^{-1} := D^{-1} - 1, \quad (162)$$

and using

$$\{\gamma_5, D^{-1}\} = 2\gamma_5,$$

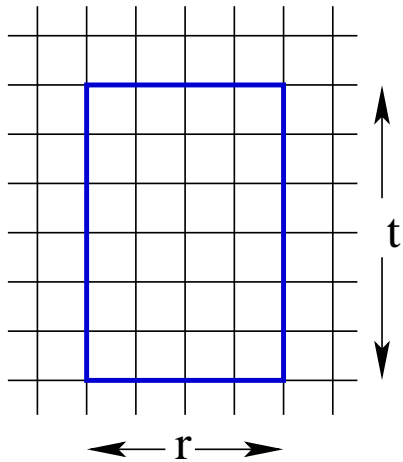
which directly follows from the Ginsparg-Wilson relation (161), we observe that \tilde{D}^{-1} acquires importance as a chiral invariant quark propagator, i.e.,

$$\{\gamma_5, \tilde{D}^{-1}\} = 0. \quad (163)$$

Constructing a chirally invariant quark propagator now boils down to the task to find an operator D which satisfies the Ginsparg-Wilson relation (161). Here, I will briefly discuss the Overlap Dirac operator [10]- [12], which was firstly introduced in the pioneering paper by Narayanan and Neuberger [10]. For these purposes, we choose

$$D = \frac{1}{2} \left[1 + \gamma_5 H \right], \quad (164)$$

Wilson loop:



(screening) masses

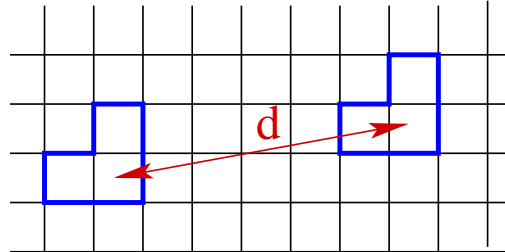


Figure 12: Wilson loop and loop-loop correlation function

where H is a Hermitian operator with eigenvalues ± 1 . A widely spread choice is

$$H = D_w / \left(D_w^\dagger D_w \right)^{1/2}, \quad (165)$$

where D_w is the standard Hermitian Wilson-Dirac operator. Inserting the choice (164) into (161), it is straightforward to prove that D (164) satisfies the Gisparg-Wilson relation. A comprehensive discussion of the quark propagator using (162) in the context of a simulation of SU(3) Yang-Mills theory can be found in [13].

5.5 Measuring observables

We have observed that the trace of the path ordered product of link variables $P(x, y)$ (132) along a closed curve C , $x = y$, is gauge invariant. Depending on the choice for the closed loop C , the expectation value of such loop variables can be connected to physical observables. For instance for the so-called Wilson loop, we choose a rectangular loop with size r in one spatial direction and the extension t in the Euclidean time direction (see figure 12). In the limit of large t , the Wilson loop expectation value is related to the potential $V(r)$ between a static quark and a static anti-quark which are separated by the distance r , i.e.,

$$\langle W[C] \rangle \propto \exp\{-V(r) t\}, \quad (166)$$

In the case that the potential is linearly rising, i.e., $V(r) = \sigma r$ (σ is called **string tension**), one would observe that the Wilson loop expectation value exponentially decreases with the area A which is encircled by the loop C . Since a linear rising quark anti-quark potential is related to confinement (see discussions below), Wilson's **area law** is a litmus test for quark confinement.

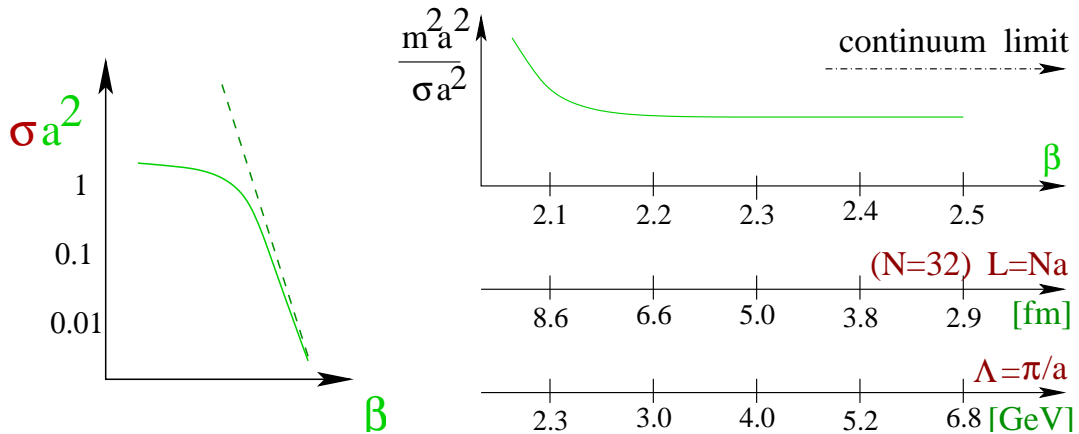


Figure 13: The continuum limit of SU(2) lattice gauge theory.

Furthermore, one can calculate the correlation function $L(t_x - t_y, \vec{x} - \vec{y})$ of two loops centred at x and y , respectively (see figure 12)). Thereby, information is transported from point x to y by gauge invariant states $|ph\rangle$. The shape of one particular loop determines its behaviour under the symmetry transformations of the underlying lattice. These symmetry transformations correspond to rotations in the continuum limit. Therefore, it is possible to select the spin quantum number of the state $|ph\rangle$ by adjusting the shape of the loop. For large distances $\Delta = t_x - t_y$, the correlation function exponentially decreases, i.e.,

$$\sum_{\vec{u}} L(t_x - t_y, \vec{u} = \vec{x} - \vec{y}) \propto \exp\{-ma \Delta\}. \quad (167)$$

Hence, the calculation of loop correlation functions provide access to the so-called **screening masses** m of physical particles. In the purely gluonic theory, the only gauge invariant states are the glue-balls, while in full QCD also hadronic states contribute to the correlation functions.

5.6 The continuum limit

For definiteness, I confine myself to the case of pure (i.e. no quarks) SU(2) gauge theory. The generalisation of the findings of the present section to $SU(N_c)$ is straightforward. The task is now to find the critical limit of the lattice Yang-Mills theory.

There is a lesson to learn from continuum Yang-Mills theory. In order to renormalise the continuum theory, one absorbs a logarithmic divergence into the bare gauge coupling. A detailed calculation yields

$$\frac{1}{g^2(\Lambda)} = \frac{11}{24\pi^2} \ln \frac{\Lambda^2}{\mu^2} + \text{finite}, \quad (168)$$

where Λ is the UV cutoff and where μ is an arbitrary renormalisation point. The coefficient in front of the logarithmic term is the quantity of interest and can be obtained by evaluating

a bunch of one-loop Feynman diagrams. Eq.(168) shows that in the critical limit $\Lambda \rightarrow \infty$ the bare coupling vanishes. This is a signal of the celebrated property of **asymptotic freedom**. Switching from the continuum to the lattice formulation, we identify $\Lambda = \pi/a$. Using $\beta = 4/g^2$, one straightforwardly derives

$$a^2(\beta) = \text{const.} \exp\left\{-\frac{6\pi^2}{11}\beta\right\}. \quad (169)$$

As a matter of asymptotic freedom, we expect the critical limit for $\beta \rightarrow \infty$. In order to search for the critical limit with the help of numerical simulations, we calculate a physical quantity, e.g. the string tension σ in units of the lattice spacing as function of the only parameter β . The outcome of such an investigation is illustrated in figure 13 (left panel). One indeed observes that the c-number σa^2 exponentially decreases for large values of β in agreement with the prediction (169) of continuum Yang-Mills theory. The quantum field theoretical limit of the classical lattice model is obtained by interpreting the correlation length, i.e., the string tension σ in the present example, as a fixed physical quantity, and reinterpreting the β dependence of the numerical data for σa^2 as the β dependence of the lattice spacing.

Let us assume we have obtained a physical mass (of e.g. a glue-ball) in lattice units, i.e., ma , as function of β . If the mass m is a physical observable, one must recover from the data the characteristic dependence $a(\beta)$ (see (169)) for sufficiently large β values. Hence, the ratio of the two dimensionless numbers $m^2 a^2 / \sigma a^2$ approaches a constant for β close to the critical point (see figure 13, right panel). Extrapolating the data to the continuum limit $a \rightarrow 0$, i.e., $\beta \rightarrow \infty$, one determines the physical mass m in units of another physical scale, i.e., $\sqrt{\sigma}$. Finally, let us count the number of parameters. The only parameter of the classical lattice model is β . However, β is no longer at our disposal in the quantum field theory limit (which implies $\beta \rightarrow \infty$). However, the physical value of the correlation length (or $\sqrt{\sigma}$ in the present example) takes over the role of a free parameter. The replacement of dimensionless parameter by mass scale in the continuum limit is a feature of many quantum field theories and is called **dimensional transmutation**. Being aware that every mass scale is obtained in units of the string tension by the lattice simulation, I will below use $\sqrt{\sigma} = 440 \text{ MeV}$ to assign the familiar units of QCD to observables. Figure 13 (left panel) shows some generic values of the UV cutoff and the physical extension for a fixed number N of grid points for direction in space time.

References

- [1] Michel Le Bellac, *Quantum and Statistical Field Theory*, Clarendon Press, Oxford.
- [2] C. N. Yang, *The spontaneous magnetization of a two-dimensional Ising model*, Phys. Rev. **85**, 808 (1952).

- [3] C. M. Fortuin and P. W. Kasteleyn, *On the Random cluster model. 1. Introduction and relation to other model*, Physica **57**, 536 (1972).
- [4] R. H. Swendsen and J. S. Wang, *Nonuniversal critical dynamics in Monte Carlo simulations*, Phys. Rev. Lett. **58**, 86 (1987).
- [5] U. Wolff, *Collective Monte Carlo Updating for Spin Systems*, Phys. Rev. Lett. **62**, 361 (1989).
- [6] Wolfhard Janke, *Nonlocal Monte Carlo Algorithms for Statistical Physics Applications*, Mathematics and Computers in Simulations **47**, 329 (1998).
- [7] K. G. Wilson, Phys. Rev. D **10**, 2445 (1974).
- [8] see e.g. D. B. Kaplan, *A Method for simulating chiral fermions on the lattice*, Phys. Lett. B **288**, 342 (1992), [arXiv:hep-lat/9206013].
- [9] P. H. Ginsparg and K. G. Wilson, *A Remnant Of Chiral Symmetry On The Lattice*, Phys. Rev. D **25**, 2649 (1982).
- [10] R. Narayanan and H. Neuberger, *A Construction of lattice chiral gauge theories*, Nucl. Phys. B **443**, 305 (1995) [arXiv:hep-th/9411108].
- [11] H. Neuberger, *A practical implementation of the overlap-Dirac operator*, Phys. Rev. Lett. **81**, 4060 (1998) [arXiv:hep-lat/9806025].
- [12] R. G. Edwards, U. M. Heller and R. Narayanan, *A study of chiral symmetry in quenched QCD using the overlap-Dirac operator*, Phys. Rev. D **59**, 094510 (1999) [arXiv:hep-lat/9811030].
- [13] F. D. Bonnet, P. O. Bowman, D. B. Leinweber, A. G. Williams and J. b. Zhang [CSSM Lattice collaboration], *Overlap quark propagator in Landau gauge*, Phys. Rev. D **65**, 114503 (2002) [arXiv:hep-lat/0202003].
- [14] G. S. Bali, K. Schilling and C. Schlichter, Phys. Rev. D **51**, 5165 (1995) [arXiv:hep-lat/9409005].
- [15] C. J. Morningstar and M. J. Peardon, Phys. Rev. D **60**, 034509 (1999) [arXiv:hep-lat/9901004].
- [16] A. Hart and M. Teper [UKQCD Collaboration], Phys. Rev. D **65**, 034502 (2002) [arXiv:hep-lat/0108022].
- [17] Z. Fodor and S. D. Katz, Phys. Lett. B **534**, 87 (2002) [arXiv:hep-lat/0104001].

- [18] Z. Fodor and S. D. Katz, JHEP **0404**, 050 (2004) [arXiv:hep-lat/0402006].
- [19] F. Csikor, G. I. Egri, Z. Fodor, S. D. Katz, K. K. Szabo and A. I. Toth, JHEP **0405**, 046 (2004) [arXiv:hep-lat/0401016].
- [20] J. Engels, F. Karsch and K. Redlich, Nucl. Phys. B **435**, 295 (1995) [arXiv:hep-lat/9408009].
- [21] K. Kajantie, M. Laine, K. Rummukainen and Y. Schroder, Phys. Rev. Lett. **86**, 10 (2001) [arXiv:hep-ph/0007109].
- [22] I. Wetzorke, F. Karsch, E. Laermann, P. Petreczky and S. Stickan, Nucl. Phys. Proc. Suppl. **106**, 510 (2002) [arXiv:hep-lat/0110132].
- [23] F. Karsch, E. Laermann, P. Petreczky and S. Stickan, Phys. Rev. D **68**, 014504 (2003) [arXiv:hep-lat/0303017].
- [24] S. Datta, F. Karsch, P. Petreczky and I. Wetzorke, J. Phys. G **31**, S351 (2005) [arXiv:hep-lat/0412037].
- [25] T. Appelquist and R. D. Pisarski, Phys. Rev. D **23**, 2305 (1981).
- [26] G. S. Bali, J. Fingberg, U. M. Heller, F. Karsch and K. Schilling, Phys. Rev. Lett. **71**, 3059 (1993) [arXiv:hep-lat/9306024].
- [27] G. S. Bali, Phys. Rept. **343**, 1 (2001) [arXiv:hep-ph/0001312].
- [28] M. Luscher and P. Weisz, JHEP **0207**, 049 (2002) [arXiv:hep-lat/0207003].
- [29] M. Luscher, K. Symanzik and P. Weisz, Nucl. Phys. B **173**, 365 (1980).
- [30] M. Caselle, R. Fiore, F. Gliozzi, M. Hasenbusch and P. Provero, Nucl. Phys. B **486**, 245 (1997) [arXiv:hep-lat/9609041].
- [31] M. Luscher and P. Weisz, JHEP **0109**, 010 (2001) [arXiv:hep-lat/0108014].
- [32] P. de Forcrand and O. Philipsen, Phys. Lett. B **475**, 280 (2000) [arXiv:hep-lat/9912050].